Bachelor Thesis

Bachelor's Degree in Industrial Technology Engineering

Power flow optimization

MEMORY

Date of submission: June 17, 2021

Author: Ignasi Ventura Nadal

Director: Eduard Bullich Massagué

Barcelona School of Industrial Engineering

Acknowledgments

To my parents, for the unconditional love and support that kept me going all these years.

To my dear grandparents, without them, I would not know where I would be.

To my family and closest friends that were always there.

A special mention to the director of this thesis, Dr. Eduard Bullich. For all the support, attention, trust, and guidance provided during the realization of this project. He opened me the doors to an entirely new topic and made it a very enjoyable and exciting process.

Summary

This thesis consists in the development of a model to optimize the operation of a hybrid power system that integrates renewable energy technologies, energy storage systems and fuel generators.

It develops a mixed-integer, non-linear, multi-period optimal power flow problem that determines how to operate the photovoltaic generators, the fuel generators, and the batteries state of charge on an hourly basis in pursuance of minimizing distribution costs. All of these variables adhering to constraints that impose the physical limitations of the system.

The problem formulates the distribution network using the Branch Flow Model for radial networks with two relaxations. It eliminates the voltage and current angles and introduces a second-order cone relaxation to convex the problem.

Furthermore, because the solution of the relaxed power flow is not guaranteed to be feasible to the non-relaxed problem, an algorithm is developed to find the optimal solution that holds the relaxation.

The implementation of this model will be made using the GAMS, MATLAB and EXCEL software and will be as generic as possible to be easily adapted to any medium voltage distribution system.

In this project, three different case studies are developed: a base scenario with photovoltaic generation and without energy storage systems, a scenario with a high level of photovoltaic penetration, and a third scenario adding batteries on the second case. All the models present a technical and economical part, and the optimization objective is to minimize the daily operating costs.

Resum

Aquesta tesi consisteix en el desenvolupament d'un model per optimitzar l'operació d'un sistema elèctric de potència que integra tecnologies d'energies renovables, generadors de combustible i sistemes d'emmagatzematge d'energia.

Desenvolupa un problema de flux de potència òptim no lineal, de programació mixta-entera i de diversos períodes, que determina com operar els generadors fotovoltaics, els generadors de combustible i l'estat de càrrega de les bateries cada hora per tal de minimitzar els costos de distribució. Totes aquestes variables s'adhereixen a restriccions que imposen les limitacions físiques del sistema.

El problema formula la xarxa de distribució mitjançant el *Branch Flow Model* per a xarxes radials amb dues relaxacions. Eliminar els angles de tensió i corrent i introduir una relaxació de con de segon ordre perquè el problema sigui convex.

A més, com que no es garanteix que la solució del flux de potència sigui factible per al problema no relaxat, es desenvolupa un algoritme per trobar la solució òptima que mantingui la relaxació.

La implementació d'aquest model es farà mitjançant el programari GAMS, MATLAB i EXCEL i serà el més genèric possible per adaptar-se fàcilment a qualsevol sistema de distribució de mitja tensió.

En aquest projecte, es desenvolupen tres casos pràctics diferents: un escenari base amb generació fotovoltaica i sense sistemes d'emmagatzematge d'energia, un escenari amb un alt nivell de penetració fotovoltaica i un tercer escenari que afegeix bateries al segon cas. Tots els models presenten una part tècnica i econòmica i l'objectiu d'optimització és minimitzar els costos operatius diaris.

Contents

List of Figures

List of Tables

Nomenclature

Sets

T Hours in a day

Γ All Grid Nodes

Γ^{S} Slack Nodes

Γ^{PV} PV Nodes

Γ^{PQ} PQ Nodes

Γ^{PQG} PQ Nodes with generation

Γ^{PQNG} PQ Nodes without generation

Ω All Grid Lines

B All batteries

Γ^{BAT} Nodes with batteries

Variables

l_{ijt} Current Squared from node i $\in \Gamma$ at node j $\in \Gamma$ and period t $\in T$ for (i,j) $\in \Omega$

M_{it} Binary Variable of the Batteries in node i $\in \Gamma^{BAT}$ and period t $\in T$

M_{rt} Binary Variable of the battery r $\in B$ and period t $\in T$

$P_{it}^{b,char}$ Charging Power at the battery of node i $\in \Gamma^{BAT}$ and period t $\in T$

$P_{it}^{b,dischar}$ Discharging Power at the battery of node i $\in \Gamma^{BAT}$ and period t $\in T$

P_{nt}^{G}, Q_{nt}^{G} Active and Reactive Power Generation at node n $\in \Gamma$ and period t $\in T$

$P_{it}^{net}, Q_{it}^{net}$ Active and Reactive Power Consumption at node i $\in \Gamma$ and period t $\in T$

P_{it}^{pv}, Q_{it}^{pv} Active and Reactive Solar Power Generation at node i $\in \Gamma^{PV}$ and period t $\in T$

P_{ijt}, Q_{ijt} Active and Reactive Power Flow from node i $\in \Gamma$ at node j $\in \Gamma$ and period t $\in T$ for (i,j) $\in \Omega$

P_{it}^{ext} External Grid Power at node i $\in \Gamma^S$ and period t $\in T$

SoC State of Charge of the battery at node i $\in \Gamma^{PV}$ and period t $\in T$

u_{nt} Square of the Voltage of node n $\in \Gamma$ and period t $\in T$

Y_{it} Binary Variable of the non Renewable Generator in node i $\in \Gamma^{PQG}$ and period t $\in T$

$\underline{I_{ijt}}$ Current from node i $\in \Gamma$ at node j $\in \Gamma$ and period t $\in T$ for (i,j) $\in \Omega$

$\underline{S_{it}^{net}}$ Net Apparent Power Consumption at node i $\in \Gamma$ and period t $\in T$

$\underline{S_{ijt}}$ Apparent Power Flow from node i $\in \Gamma$ at node j $\in \Gamma$ and period t $\in T$ for (i,j) $\in \Omega$

$\underline{V_{nt}}$ Voltage of node n $\in \Gamma$ and period t $\in T$

Parameters

η Battery charging and discharging efficiency

C_i Maximum Solaar Power that can be supplied at node i $\in \Gamma^{pv}$

Cap_m^{bat} Rated Energy at battery m $\in B$

$ERates_t$ Electrical rates at period t $\in T$

F_t^{pv} Day-ahead Forecast of the available solar power at node i $\in \Gamma^{pv}$ and period t $\in T$

I_{ij}^{mx} Maximum electric current from node i $\in \Gamma$ at node j $\in \Gamma$ and period t $\in T$ for (i,j) $\in \Omega$

P_{nt}^C, Q_{nt}^C Active and Reactive Power Consumption Forecast at node n $\in \Gamma$ and period t $\in T$

P_n^{Gmn}, Q_n^{Gmn} Minimum Active and Reactive Power Generation at node n $\in \Gamma^{PQG}$

P_n^{Gmx}, Q_n^{Gmx} Maximum Active and Reactive Power Generation at node n $\in \Gamma^{PQG}$

r_{ij}, x_{ij} Resistance and Reactance of the line (i,j) $\in \Omega$

SoC_i Initial State of Charge of the battery at node i $\in \Gamma^{PV}$

V_n^{mx}, V_n^{mn} Maximum and Minimum Squared Voltage of node n $\in \Gamma$

$\underline{V_n^{slack}}$ Voltage of node n $\in \Gamma^S$

$\underline{z_{ij}}$ Line Impedance from node i $\in \Gamma$ at node j $\in \Gamma$ for (i,j) $\in \Omega$

Acronyms

BESS Battery Energy Storage Systems.

BFM Branch Flow Model.

DN Distribution Network.

DRES Distributed Renewable Energy Sources.

DSO Distribution System Operator.

GA Genetic Algorithm.

GAMS General Algebraic Modeling System.

IEEE Institute of Electrical and Electronics Engineers.

MVDN Medium Voltage Distribution Network.

OPF Optimal Power Flow.

SCIP Solving Constraint Integer Programs.

SoC State of Charge.

1 General Introduction

1.1 Organization of this thesis

This thesis consists of eight sections. This first one is an introduction to the project and its purposes.

The second section defines the state of the art. It summarizes the actual situation of electrical power systems and presents the power flow study as a numerical tool to analyze the system. Then it briefly introduces the convex mathematical optimization followed by the definition of the optimal power flow problem.

The third section formulates the base power flow equation for a generic MVDN for a single period, using the Branch Flow Model. Then it models the three components that will be applied in the case studies: battery energy storage systems, non-renewable power generators, and photovoltaic generators.

The fourth section is the definition of the multi-period optimal power flow problem. Firstly, it develops the equations introduced in the previous chapter, redefining them to the solver's notation and making them more efficiently calculated. Secondly, it introduces the time set to all the equations. Then it also combines the network's variables with the components' variables. Once the power flow is defined, it develops the objective function of the problem. The last two subsections introduce the relaxation of the problem and its implementation into the software, respectively.

The fifth section comprises the application of the multi-period optimal power flow. It has two parts. The first one introduces the parameters of the network. The second one presents the results of three different case studies. A solution recovery algorithm is developed in this scenario to find feasible results for the non-relaxed problem. The sixth section presents the conclusions of the results of the three scenarios.

Finally, the seventh and eighth sections explain the economic analysis and the environmental impact of this thesis.

1.2 Objectives and scope

The main objective of this thesis is to study how different capabilities of photovoltaic generation and the use of battery energy storage systems affect the operation of a medium voltage distribution network.

Several cases combining different solar panel rated powers with the implementation or not of batteries are reviewed through a multi-period optimal power flow with fuel generators. These scenarios will provide the variables' value to see what are the main differences between each case. How much varies the daily operation cost, when the solution provided by the solver is feasible, how the system's variables evolve in the peak production hours, when is renewable production curtailed, et cetera. These are some of the main factors compared in the following chapters.

In this project, the power flow equations will be developed following the Branch Flow Model, adding when stated the fuel generation, the solar generation, and the energy storage systems technical and economic model. Also, the exchange through the slack node with the external grid will be allowed, only constrained by the physical limits. All constituting an optimal power flow problem that will minimize the daily operating costs. The model will assume that all the inputs are deterministic.

Because some equations of the model will be relaxed to ensure the convergence of the optimization, the problem will not always be feasible to the non-relaxed model. Another goal of the thesis will be to develop an algorithm that guarantees that the solver can find the optimal solution that satisfies all the power flow equations.

The optimization will be done with the GAMS software, adapting all the model equations into its programming language. The MATLAB software will also be used to define, post-process and analyze the data and the EXCEL software will be used to define and plot the results.

The model formulation will take as a basis a GAMS file and various MATLAB files provided by Dr. Bullich. These files contain a simple optimal power flow formulation with distributed diesel generation for one period and the files to interface both software.

2 State of the Art

2.1 Actual Situation

The main goal of an existing electrical power system is to uninterruptedly satisfy the power demanded by all customers efficiently and reliably. To achieve this, it must find a proper method of interconnecting the generating resources and the customers' loads. Because the power industry has been in a changing environment since its start, engineers are continuously creating new techniques and analysis methods to address this goal.

Since the firsts electrical networks in the late 19th century, the electricity supply industry has experienced a continuous transformation worldwide. It went from very simple distribution lines with the generator located not far away from the load to massive distribution networks that integrate enormous distances between loads, different types of generation, and enormous demands of electricity. [Ene]

This unprecedented change is fundamentally due to an ever-increasing demand for electricity that the world has experienced since the discovery of electricity generation, especially in developed countries. In the following Figure 1 is shown the electricity consumption evolution of the United States created by the Energy Information Administration. The 4 trillion kilowatt-hours that this country consumes nowadays is more than eight times the use of electricity from 60 years ago. It is important to note that this booming has been in all sectors, especially in residential and commercial use. [Age20] Moreover, the growth represented in the subsequent graph is the same that happened in Europe and other industrialized countries. [GK17]

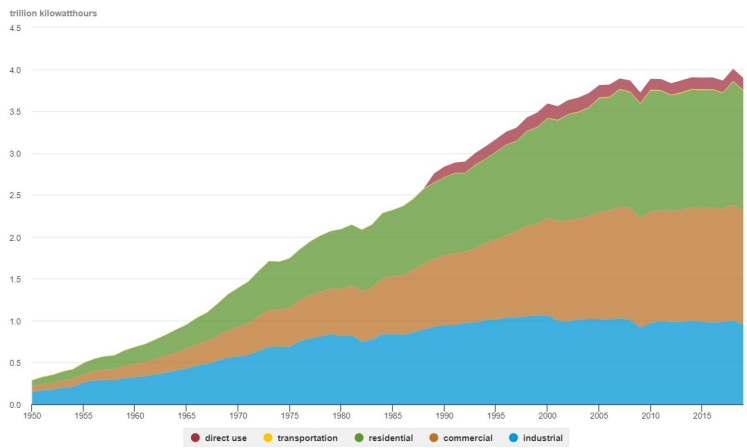

Figure 1: U.S. Electricity Consumption Evolution (Source: EIA)

Another critical aspect that has boosted this evolution is the search for profitability. Electrical companies have continually been developing new techniques and inventing new devices and methods to reduce power losses and distribution costs.

Finally, the widespread support for using environment-friendly energy sources in order to reduce carbon dioxide emissions due to global warming is boosting the electricity market. Scientists have developed the technology to obtain clean energy from the sun, wind, and water to electricity. [Ass20] These new ways of generating power are replacing fossil fuel generators, with the new challenges that imply to the distribution networks because of the continuous changes in the environment.

No electrical power system is an exact copy of another one. They involve many varying parameters such as the size, the topography, the generating resources available, the structural components, et cetera. However, they all can be divided into three subsystems that condition the overall system: generation, transmission, and distribution. This is represented in Figure 2. Firstly, there are generators, which can be from many different power plants such as nuclear, hydroelectric, solar, along with others. Followed by a step-up transformer, which increases the output voltage of the line reducing the output current. The purpose of the transformer is to reduce the power losses in the transmission line. The basic theory behind this is that the power losses of a line can be expressed as $P = RI^2$, R being the line resistance, so by reducing the current, a lot of the dissipated energy can be reduced. Then there are the transmission lines to transport the power generated, and then the step-down transformer that reduces the voltage to an acceptable level for distribution. Finally, there are the distribution networks that provide the energy to the consumers.

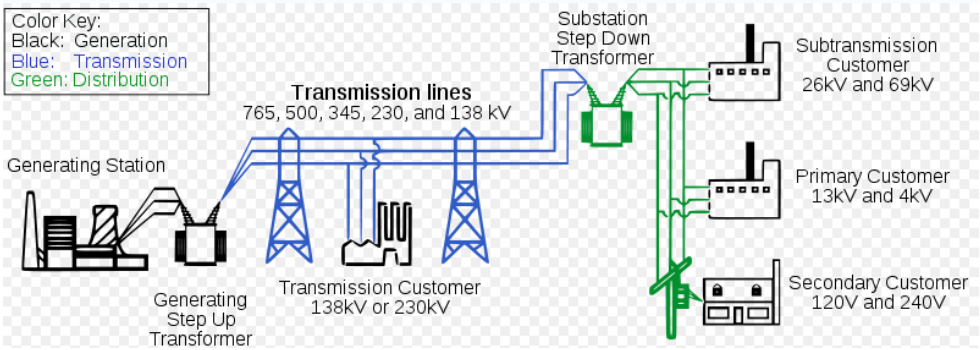

Figure 2: Simplified diagram of AC electricity delivery from generation stations to consumers' service drop. [fL12]

All the variability that exists in each distribution network, the complexity of the global system, and the flexibilities of each model all in a very competitive environment, which is the electricity supply business, requires a potent tool to assess the planning and operation of the system. This is quite effectively achieved with extensive power flow and derived studies.

2.2 Power Flow Study

In power engineering, the Power Flow Study, or Load Flow Study, is a quantitative study to determine the flow of electric power in a distribution network under given load conditions. It provides a non-linear system that helps engineers describe the energy flow through a transmission line. The study must guarantee the feasibility of the power flow solution to apply costs theory and optimize the system's stability, as well as for optimization purposes. [Mom09]

The main objective is to know various AC power parameters such as the voltages at each bus, the line current flows, and system losses given a description of the network, the loads of each bus, and the generation data. In more simple words, the objective of the power flow is to determine the steady-state operating values of an electrical distribution network. [Alb19]

This is a problem of great engineering complexity. Firstly, the model must take into account a lot of variables and restrictions imposed not only by the fundamental laws of electricity but for the physical characteristics of each transmission line, such as thermal and stability limits. [Ach+04] Secondly, the distribution networks are becoming more challenging of operating and planning because of the increasing demand for electricity and its flexibility. Lastly, the new challenges of using renewable resources as electricity generators imply integrating them into the network.

These studies are frequently used for planning, control, and operations of a working DN and to plan future expansions on DN such as new loads or new generating stations. Additionally, the power flow problem supports an even more potent tool used for optimization in DN. For example, the PF could be used to create models to optimize, given a load forecast for each bus, which generators the network should use and when they should be used in order to reduce the power losses. Or given a solar power forecast, which should be the state of charge of each battery at every hour if the problem wants to minimize the solar curtailment costs. Basically, it can be used as a tool to improve the system performance under given operating conditions.

Unsurprisingly, there are numerous possibilities for finding the best decision regarding the different variables in each DN to have a more efficient, secure, and robust power system. This thesis will study how to determine the appropriate operating steady-state conditions with optimal power flow solution methods. The strategy requires a concrete and reliable modelling of the system and a potent optimization solver.

These optimal feeder flow problems have increased their usefulness over the last few years due to the fact that the networks are converting from passive systems to active ones. The rise in demand management and installation of active elements in the distribution grid like photovoltaic panels and batteries have provided the power systems control variables that can be adjusted. Before jumping into these types of problems, the optimization techniques are presented.

2.3 Optimization

This section pretends to be a small introduction to convex mathematical optimization and its types. It is geared towards later introducing its application to the optimal power flow algorithm. [Ber14] [BV04]

The convex optimization addresses the general problem of minimizing or maximizing a convex function in a feasible convex set. A simplified generic model would be the following:

$$min\ f(x_n) \tag{2.1}$$

$$subject\ to: g_i(x_n) \leq b_i\ and\ h_j(x_n) = d_j \tag{2.2}$$

Where $f(x_n)$ in (2.1) refers to the function that to minimize or maximize, the objective function. The vector $x = (x_1, ..., x_n)$ is the optimization variable of the model. The functions $g_i(x_n)$ for $i = 1, ..., m$ are the set of inequality constraints and $h_j(x_n)$ for $j = 1, ..., p$ are the set of equality constraints. Finally, the vectors b_i and d_j in (2.2) are the bounds of the constraints.

The solution of this model would be the vector x_n^* that has the smallest objective value while satisfying all the constraints. [Ber14] [Sor17]

For the problem to be convex optimization, the objective and constraint functions must be convex. All of them must satisfy the equation

$$f_i(\alpha x + \beta y) \leq \alpha f_i + \beta f_i \tag{2.3}$$

for all $x, y \in \mathbb{R}^n$ and $\alpha, \beta \in \mathbb{R}$ with $\alpha + \beta = 0$, $\alpha \geq 0$, $\beta \geq 0$. [BV04]

The main reason why the convexity of the model is so crucial in optimization is that it guarantees that the local minimum or maximum point is also the global one and that this point is unique. This fact is what allows these optimization problems to be solved up to an immense size efficiently. If the condition (2.3) is not met, the problem would have multiple feasible regions and multiple local optimal points. It would need much more computing time to determine a global optimum or the infeasibility of the model, and the time could increase exponentially depending on the number of variables and constraints. [BV04]

2.3.1 Optimization Classification

There are a lot of different types of optimization problems. They can be grouped in a large variety of classes with the most important types in Table 1, with each one having a different approach and solving techniques. However, the main classification question is if whether the model has linear or non-linear equations. [LY08]

Programming Types	
Acronym	Definition
LP	Linear Program
IP	Integer Program
MIP	Mixed-Integer Program
MILP	Mixed-Integer Linear Program
NLP	Non-Linear Program
QP	Quadratic Program
QCP	Quadratically-Constrained Program
SOCP	Second Order Cone Program
MISOCP	Mixed-Integer Second Order Cone Program

Table 1: Common programming types

When f, g_i and h_j are linear it generates a linear optimization problem. This is the easiest model since the mathematics are more evident, the theory is very developed, and it requires very little computation time. They are also more accessible because the linearity of the equations guarantees the convexity of the model since all linear equalities satisfy (2.3).

The IP appears when all the variables in the problem are constrained to be integers. If not all the decision variables are discrete, then it is a MIP. Finally, the MILP involves problems with discrete and continuous decision variables and with all the equations linear.

If at least one equation in the model is non-linear, then it converts to an NLP. In that case, the difficulty of the problem increases and different and more complex algorithms than with linear models are needed. For this reason, engineers have come up with lots of strategies to linearize equations without excessively compromising the model. Nevertheless, because of the vast practical engineering applications that non-linear problem solutions have, lately, many improvements have been made to tackle this issue.

QP is one of the simplest NLP, where the objective function is a second-order polynomial and the constraints are linear. QCP appears when a constrained equation has a second-order term.

Finally, the last type introduced is the Second-Order Cone Program. For the model to be a SOCP a restriction must have a Lorentz cone structure. A simple example in $\mathbb{R}^3$ would be $\{(x, y, z)|\sqrt{x^2 + y^2} \leq z\}$. A geometric interpretation is shown in Figure 3.

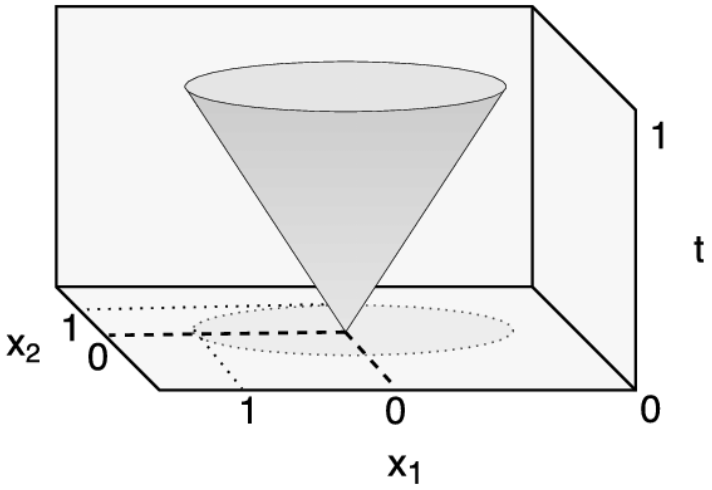

Figure 3: Second Order Cone [Bha16]

The generic model would be as follows:

$$min\, c^T x_n \tag{2.4}$$

$$subject\, to:\ ||A_i x_n + r_i||_2 \leq b_i^T x_n + e_i \quad and \quad h_j x_n = d_j \tag{2.5}$$

Where $||x||_2$ indicates Euclidean norm and ^{T} indicates transpose. As before, x are the optimiza-

tion variables and the rest are problem parameters.

MISOCP only means that the SOCP has continuous and discrete decision variables. The mixed-integer problem with second-order cone equations will be the type used in this thesis.

2.4 Optimal Power Flow

As previously seen, determining the steady-state operating condition of a network is a very complex task. There are many constantly changing variables and parameters that could make the operator work impossible if it was not for the computation software.

What initially could be done with only the observation and the experience of an operator, now has turned into a very complex task that needs numerical optimization techniques and state-of-the-art computer technology. One of the most used techniques nowadays is the OPF.

The optimal Power Flow model represents the problem of determining the best-operating settings of an electric power system while meeting the demand given throughout a transmission network and trying to minimize the operation costs. [Mom09]

The idea of the OPF was firstly introduced in the early 1960s by Carpentier [Gar04] and can be easily understood if one thinks of the conventional power flow study. Instead of aiming to determine the operating condition, the point is to determine the most favourable operating settings corresponding to an objective function. This function usually incorporates economic, security, and environmental aspects.

Hence, in this method, the power flow model is formulated with all the characteristics of the DN but distinguishing the fixed parameters from the control variables that can be adjusted. For example, the current limit of a line would be a fixed parameter and the power generation at each node could be a control variable.

Once applied this model with its constraints into an optimization solver, an objective function is needed to find the optimum variable values that minimize or maximize this function.

Table 2 presents some examples of the most common functions used nowadays. There are many options and the functions can be combined. However, choosing this function cannot be arbitrary and must be done with a meticulous analysis of the system security and economy.

In the Table 2 are also some examples of typical constraints of power systems. These constraints are always to be satisfied if the solution is to exist. If any of these limits are not met, then the solution would be unfeasible.

Examples of Objectives functions and Constraints	
Objective functions	Constraints
Economic Dispatch	Limits on control variables
Environmental Dispatch	Current limits on the lines
Minimum line power Losses	Voltage limits at each bus
Minimum Deviation from a target schedule	Generation outputs
Minimum Non-renewable sources use	Batteries capacity
	Photovoltaic maximum power

Table 2: Examples of objectives and constraints Commonly found in OPF [Mom09]

2.4.1 Challenges and justification of the work

The electric power market has been increasing since its beginning and is projected to do so for some years. Moreover, recently this tendency has even got more traction with the climate change action and the use of renewable sources such as photovoltaic energy or wind energy.

However, these new energy sources pose a new challenge in power generation because of their variability. The generated power cannot be controlled at any given time, like with fossil or nuclear sources. The weather is constantly changing, and it is difficult to predict it more than a few hours away. Therefore some changes in the power networks must be applied if they are to use these carbon-neutral resources on a large scale.

This work proposes a model that integrates a renewable source as photovoltaic energy and analyzes how a power system will respond given different scenarios.

Solar energy also has the problem that, unlike wind energy, it is only available for a few hours in the day. Hence it can be easily understood that if a network only relied on this resource, the night demand or the demand on a cloudy day could not be supplied. Also, to balance the energy supply and demand, there could be moments where solar energy production has to be reduced not to exceed the electricity demand. So to address this issue, a model where energy storage systems are applied is proposed.

3 Power Flow Formulation in radial DN

This section will introduce the equations that characterize a medium voltage distribution network operated in a radial configuration with photovoltaic generation, batteries, and demand flexibility.

3.1 DN Modelling

This subsection intends to be an introduction to how this thesis will be modelling the power system.

Consider a graph representing a power network as $G(N, E)$ where N represents the buses and E represents the nodes' links. The network will be radial if G has a tree structure, meaning there are no closed loops in the grid topology. A typical example would be Figure 4. As it can be seen, one bus delivers power to the next one without the possibility of reaching an original bus unless the power turns backwards. This kind of topology is the cheapest and most straightforward to operate. Its major drawback is that, if for some reason a bus is disconnected, all the buses downstream get disconnected too. [FL12]

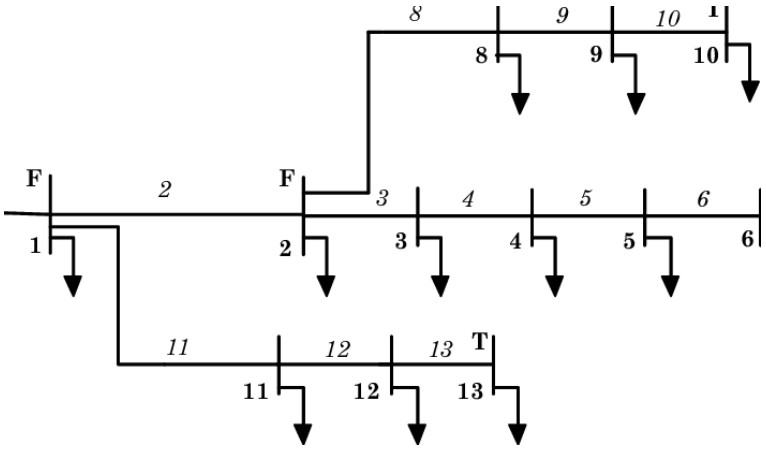

Figure 4: Diagram of a typical radial distribution system [SS04]

This kind of grid topology permits applying the power flow equations in a recursive structure that facilitates computing, such as the Branch Flow Model, first developed in [BW89]. This model will establish the formulation used from now on for the analysis and optimization of the MVDN.

The notation used in the power flow formulation will be as follows:

- The nodes N of the power network are defined by an $i \in N$, a $j \in N$ or a $k \in N$.
- The links E between nodes are defined by a upstream node i and a downstream node j, $i, j \in E$.
- For each link, let $\underline{z_{ij}} = r_{ij} + ix_{ij}$ be the line resistance, let $\underline{S_{ij}} = P_{ij} + iQ_{ij}$ be the sending-end complex power and let $\underline{I_{ij}}$ be the complex current.
- For each node, let $\underline{V_i}$ be the complex voltage, let $\underline{y_j} = g_j + ib_j$ be the complex admittance and let $\underline{s_i}$ be the power injection.
- In this chapter, the formulation will be considered only for a single period for simplification reasons, so the time set will not be taken into account. Nevertheless, in posterior chapters a multi-period formulation for OPF will be used.

All the variables must satisfy the Ohm's law (3.1), which defines the downstream node voltage as the upstream node voltage minus the voltage drop.

$$\underline{V_i} - \underline{V_j} = \underline{z_{ij}}\,\underline{I_{ij}}, \qquad \forall (i,j) \in E \tag{3.1}$$

The branch power flow equation (3.2) expresses the apparent power of the line.

$$\underline{S_{ij}} = \underline{V_i}\,\underline{I_{ij}^*}, \qquad \forall (i,j) \in E \tag{3.2}$$

The power balance at each bus (3.3) establishes that the power injection at each node must be the difference between the incoming power from upstream nodes and the leaving power to downstream nodes and adding the effect of the transverse components of the network. These effects will be ignored in the OPF since it has minimal effect on the voltages. The power losses are aggregated to the upstream power flow. [Mas18][Vic19]

$$\sum_{k:j\to k} \underline{S_{jk}} - \sum_{i:i\to j} (\underline{S_{ij}} - \underline{z_{ij}}|\underline{I_{ij}}|^2) + \underline{y_j^*}|\underline{V_j}|^2 = \underline{s_j}, \qquad \forall (i,j),\,(j,k) \in E \tag{3.3}$$

This power balance (3.3) does not apply to the first node of the DN. Because the losses are defined aggregated to the upstream flow, in the border node the power losses are external. So the power balance for the limit buses is expressed in the following equation (3.4).

$$\sum_{j} \underline{S_{ij}} = \underline{s_i}, \qquad i = 1; \quad \forall j \in N \tag{3.4}$$

The equations (3.1), (3.2), (3.3) and (3.4) are the ones that define the BFM. [FL12]

3.2 Battery Energy Storage Systems

The battery is an energy storage system that uses electrochemical cells to store energy chemically. Their applications in DN have been studied for some years with some pilots on the way around the world. The energy storage necessity in the power supply industry mainly appears because the DRES can only supply electricity during specific periods during the day and they can also become useless for a few days. There can also be a curtailment problem during certain times of the day. Therefore, the installation of energy storage systems in power systems can provide great value for the end-user, the electricity companies, and the distribution system.

There are currently many battery modelling types used, and a lot of research and improvements are being made on the topic because of the increasing need for battery energy storage systems. There are from very extensive and complex electrochemical formulations to high-level stochastic models. [JH08] However, the purpose of the system is what determines the best-suited model, which in this case will be for network operational analysis. Thus, the model developed will not focus on how the batteries internally work but on their applications to the network's behaviour.

In this thesis, the model will consist of the following parameters: the battery capacity, the battery power limits, the charging and discharging efficiency, and the initial state of charge. It will assume that the charging and discharging efficiency is identical to simplify the formulation.

Since the model is developed for operational planning, it will assume that the SoC upper and lower limits do not depend on the lifetime of the battery, so they will remain constant. Nevertheless, future modifications in these limits are to be considered in future planning. [Swa17]

The model that follows is based on a linear formulation proposed in [Clo+19] by the CITCEA-UPC.

The capacity of the batteries is measured in kWh and provides an approximation of the total amount of energy that can be stored in them. The battery power limits are established by the manufacturer and are measured in kW. The operation efficiency is an approximation of the power losses there are in the batteries in the energy conversions. The initial state of charge provides the information of the level of charge of each battery relative to their total capacity and is stated in p.u. [Clo+19]

The BESS will be expressed with the equations (3.5) and (3.6).

$$SoC(t) = SoC(t-1) + \eta\, P_t^b \frac{\triangle t}{Cap^{bat}}, \qquad \forall t \in T \quad (P_t^b \geq 0) \tag{3.5}$$

$$SoC(t) = SoC(t-1) + \frac{1}{\eta}\, P_t^b \frac{\triangle t}{Cap^{bat}}, \qquad \forall t \in T \quad (P_t^b \leq 0) \tag{3.6}$$

As can be seen, the model needs two variables to characterize the system. One being the charge and discharge power of the battery and the other being the state of charge of the battery at each period.

Equations (3.5) and (3.6) define the state of charge of the current interval by adding two terms. The first one is the SoC from the previous period and the second term adds or subtracts energy from the battery depending on if the battery is charging or discharging.

The value of the SoC in the first period of the device is equal to the initial state of charge defined in the parameters.

$$SoC\,(t=0) = SoC_i \tag{3.7}$$

The model also needs to consider some variable restrictions. The SoC is between 0 and 1 p.u., which will be its storage limits in (3.8). The maximum ramp of charge and discharge will also be restricted with the following equations (3.9) and (3.10).

$$0 \leq SoC\,(t) \leq 1, \qquad \forall t \in T \tag{3.8}$$

$$P_t^b \leq P_{mx}^b, \qquad \forall t \in T \quad (P_t^b \geq 0) \tag{3.9}$$

$$-P_{mx}^b \leq P_t^b, \qquad \forall t \in T \quad (P_t^b \leq 0) \tag{3.10}$$

In preparation to apply the algorithm in the GAMS software, the following adaptations are implemented.

It will consider two positive variables representing the charging and discharging power instead of one free variable. This allows to formulate the SoC of the batteries in a single equation (3.11) and also will simplify the task of post-processing the results.

A binary variable M_t is also applied in the new charge and discharge power limits. The objective of this variable is to block the possibility of getting a solution where the battery is simultaneously charging and discharging. The final restrictions are formulated in (3.12) and (3.13).

$$SoC(t) = SoC(t-1) + \eta\, P_t^{b,char} \frac{\triangle t}{Cap^{bat}} - \frac{1}{\eta}\, P_t^{b,dischar} \frac{\triangle t}{Cap^{bat}}, \qquad \forall t \in T \tag{3.11}$$

$$0 \leq P_t^{b,char} \leq M_t P_{mx}^b, \qquad \forall t \in T \tag{3.12}$$

$$0 \leq P_t^{b,dischar} \leq (1 - M_t) P_{mx}^b, \qquad \forall t \in T \tag{3.13}$$

All the variables and parameters of the proposed formulation are shown in the following Table 3.

Variables	Definition	Units
$SoC(t)$	State of Charge of the Battery	p.u.
$P_t^{b,char}$	Power entering the battery	p.u.
$P_t^{b,dischar}$	Power exiting the battery	p.u.
M_t	Charging/Discharging the battery	/
Parameters	**Definition**	**Units**
P_{mx}^b	Maximum Power that the battery can store or discharge	p.u.
Cap^{bat}	Rated Energy of the battery	p.u.
η	Charging and discharging efficiency	p.u.

Table 3: Variables and parameters of the battery model

3.3 Non-Renewable Power Generation

Although engineers are getting closer to achieving a fully renewable power generation in a DN, the truth is that it might take some years to achieve it. So, in the meantime, networks still need to rely on non-renewable sources in order to satisfy all the demand.

In this thesis, the non-renewable power production will be modelled with diesel generators. It will use a positive variable, a free variable and one binary variable to formulate this electricity source.

The positive variable will be the active power provided by each generation, the free variable will be the reactive power provided by each generator, and the binary variable will represent the state of the generator, whether it is on or off.

The problem also needs to consider active and reactive power limits for the generators. The maximum active power produced is defined by the rated capacity of the generator. The minimum active power also needs to be constrained in order to represent the generators' minimum

operating range. This minimum is introduced following the manufacturer's recommendations to prevent the generators from operating at too low a load. The manufacturers also set the reactive power generation limits. As done in the BFM, the formulation of the model will be without the time set, although it will be added in the Optimal Power Flow. [DC19]

$$P_i^G \leq P_i^{Gmx} Y_i, \qquad \forall i \in \Gamma^{PQG} \tag{3.14}$$

$$P_i^{Gmn} Y_i \leq P_i^G, \qquad \forall i \in \Gamma^{PQG} \tag{3.15}$$

$$Q_i^G \leq Q_i^{Gmx} Y_i, \qquad \forall i \in \Gamma^{PQG} \tag{3.16}$$

$$Q_i^{Gmn} Y_i \leq Q_i^G, \qquad \forall i \in \Gamma^{PQG} \tag{3.17}$$

All the variables and parameters of the proposed formulation are shown in the following Table 4.

Variables	Definition	Units
P_i^G	Active Power Generation	p.u.
Q_i^G	Reactive Power Generation	p.u.
Y_i	Connection /Disconnection of the Generator	/
Parameters	**Definition**	**Units**
P_i^{Gmx}	Maximum Active Power Generation	p.u.
Q_i^{Gmx}	Maximum Reactive Power Generation	p.u.
P_i^{Gmn}	Minimum Active Power Generation	p.u.
Q_i^{Gmn}	Minimum Reactive Power Generation	p.u.

Table 4: Variables and parameters of the non-renewable generation model

3.4 Photovoltaic Generation

The photovoltaic cell is an electronic device used to generate electricity from photons. It is based on a chemical and physical phenomenon called the photovoltaic effect. Photons hit the surface of a semiconductor material such as silicon, which sets electrons free from the nucleus. The result is a direct current (DC) flow that, using power electronics, can be converted into alternating current (AC). [Işı15]

There are a lot of types and models for photovoltaic cells. This thesis, however, will not focus on how to formulate the power produced but rather on how it affects the power network.

The problem will use two variables to calculate the active and reactive power generation based on two parameters. The maximum energy that can be supplied by the solar power station and a day-ahead forecast of the power available at each period.

Reactive power compensation is modelled as a flexibility of the photovoltaic generation, carried out by power electronic interfacing equipment. The reason being to follow the actual European guidelines for MVDN, where the reactive power is between a generation of 40 % of the active power injected to a 35 % consumption. [RAW14] [Swa17]

$$P_{it}^{pv} \leq F_t^{pv} C_i, \qquad \forall i \in \Gamma^{PV} \quad \forall t \in T \tag{3.18}$$

$$-0.35 P_{it}^{pv} \leq Q_{it}^{pv} \leq 0.4 P_{it}^{pv}, \qquad \forall i \in \Gamma^{PV} \quad \forall t \in T \tag{3.19}$$

All the variables and parameters of the proposed formulation are shown in the following Table 5.

Variables	Definition	Units
P_i^{pv}	Active Photovoltaic Power Generation	p.u.
Q_i^{pv}	Reactive Photovoltaic Power Generation	p.u.
Parameters	**Definition**	**Units**
F_t^{pv}	Maximum Solar Power Generated	p.u.
C_i	Day-ahead Forecast Solar Power	p.u.

Table 5: Variables and parameters of the photovoltaic generation model

4 Formulation of the Optimal Power Flow

4.1 Optimal Power Flow Formulation

The section introduces the optimal operation of a feeder flow minimizing the operating costs of a radial network incorporating the models developed in the previous chapter. All the variables and parameters will use a per-unit system (p.u.) unless it is contrarily specified.

The following assumptions will be made:

1. The model will be working with a single-line representation of the MVDN. Therefore, it will consider the distribution system balanced across its three phases. For unbalanced systems, multiple phase modelling would be needed.

2. The loads and generation in each bus are considered to be aggregated.

3. Three types of nodes will be considered: $slack$, PV and PQ. The slack node represents the limit between the transmission network and the distribution network.

4. As previously stated in the power flow formulation, the transverse components of the network will be ignored since they have negligible effects on the voltages when the DN is working in normal conditions.

5. The problem will be formulated as a multiperiod with 24 periods representing a full-day operation.

The Branch Flow Model equations (4.1) - (4.4) are explained in the previous chapter. Down below are redefined to the OPF nomenclature adding the time period set.

$$\underline{V_{it}} - \underline{V_{jt}} = \underline{z_{ij}}\,\underline{I_{ijt}}, \qquad \forall (i,j) \in \Omega\,; \quad \forall t \in T \tag{4.1}$$

$$\underline{S_{ijt}} = \underline{V_{it}}\,\underline{I^{*}_{ijt}}, \qquad \forall (i,j) \in \Omega\,; \quad \forall t \in T \tag{4.2}$$

$$-\sum_{k:j\to k} \underline{S_{jkt}} + \sum_{i:i\to j} (\underline{S_{ijt}} - \underline{z_{ij} {I_{ijt}}^{2}}) = \underline{S^{net}_{it}}, \qquad \forall (i,j),\,(j,k) \in \Omega\,; \quad \forall j \in \Gamma \setminus \{1\}; \quad \forall t \in T \tag{4.3}$$

The power balance for a slack node is indicated in equation (4.4).

$$\sum_{j} \underline{S_{ijt}} = \underline{S^{net}_{it}}, \qquad \forall i \in \Gamma^{S} \quad \forall (i,j) \in \Omega; \quad \forall t \in T \tag{4.4}$$

The slack voltage is fixed by the transmission line as shown in (4.5).

$$\underline{V_{nt}} = \underline{V_n^{slack}}, \qquad \forall n \in \Gamma^S\,; \quad \forall t \in T \tag{4.5}$$

A reformulation of the equations (4.2) and (4.3) will be used in order to linearize the model. Non-linear expressions complicate the problem greatly and highly increase the computing time. Therefore the following variable changes are proposed in (4.6) and (4.7).

$$I_{ijt}^2 = l_{ijt}, \qquad \forall (i,j) \in \Omega\,; \quad \forall t \in T \tag{4.6}$$

$$V_{nt}^2 = u_{nt}, \qquad \forall n \in \Gamma\,; \quad \forall t \in T \tag{4.7}$$

Also, because the optimization solvers do not work with complex numbers, they will be reformulated. Hence equation (4.4) will be used as (4.8) and (4.9).

$$\sum_j P_{ijt} = -P_{it}^{net}, \qquad \forall i \in \Gamma^S\,; \quad \forall t \in T \tag{4.8}$$

$$\sum_j Q_{ijt} = -Q_{it}^{net}, \qquad \forall i \in \Gamma^S\,; \quad \forall t \in T \tag{4.9}$$

Equation (4.5) is redeveloped in (4.10) using the variable changes.

$$u_{nt} = (V_n^{slack})^2, \qquad \forall n \in \Gamma^S\,; \quad \forall t \in T \tag{4.10}$$

The power balance for all the PV and PQ buses will also need to be expressed in two equations, (4.11) and (4.12).

$$P_{jt}^{net} = \sum_i (P_{ijt} - r_{ij} l_{ijt}) - \sum_k Pjkt, \qquad \forall (i,j),\,(j,k) \in \Omega\,; \quad \forall j \in \Gamma \setminus \{1\}\,; \quad \forall t \in T \tag{4.11}$$

$$Q_{jt}^{net} = \sum_i (Q_{ijt} - x_{ij} l_{ijt}) - \sum_k Qjkt, \qquad \forall (i,j),\,(j,k) \in \Omega\,; \quad \forall j \in \Gamma \setminus \{1\}\,; \quad \forall t \in T \tag{4.12}$$

The voltage drops, taking into account the variable change in equation (4.7), will be formulated as in (4.13).

$$u_{jt} = u_{it} - 2(r_{ij} P_{ijt} + x_{ijt} Q_{ijt}) + l_{ijt}(r_{ij}^2 + x_{ij}^2), \qquad \forall (i,j) \in \Omega\,; \quad \forall t \in T \tag{4.13}$$

This (4.13) equation is the Ohm's law formula developed so that it is linearized and has not any complex variables or parameters.

To do so, the Ohm's law is squared, obtaining the following expression (4.14). Then the apparent power definition is reformulated as in (4.15). The last two terms of the equation (4.15) can be rewritten as (4.16), obtaining the proposed voltage drops equality in (4.13).

With this last reformulation, the Ohm's law is applied as a linear, non-complex equation. However, the complexity is hidden under the squared variables.

$$u_{jt} = u_{it} + |z_{ij}|^2 \, l_{ijt} - \underline{z_{ij} I_{ij}} \underline{V_{it}^*} - \underline{z_{ij}^* I_{ij}^*} \underline{V_{it}}, \qquad \forall (i,j) \in \Omega\,; \quad \forall t \in T \tag{4.14}$$

$$u_{jt} = u_{it} + |z_{ij}|^2 \, l_{ijt} - \underline{z_{ij}} \underline{S_{ij}^*} - \underline{z_{ij}^*} \underline{S_{ij}}, \qquad \forall (i,j) \in \Omega\,; \quad \forall t \in T \tag{4.15}$$

$$\underline{z_{ij}} \underline{S_{ij}^*} + \underline{z_{ij}^*} \underline{S_{ij}} = 2 r_{ij} P ij + 2 x_{ij} Q_{ij}, \qquad \forall (i,j) \in \Omega\,; \quad \forall t \in T \tag{4.16}$$

Finally, the apparent power flow of the line equation will be enunciated in the expression (4.17).

$$l_{ijt} = \frac{P_{ijt}^2 + Q_{ijt}^2}{u_{it}}, \qquad \forall (i,j) \in \Omega\,; \quad \forall t \in T \tag{4.17}$$

Expression (4.17) comes from the squared apparent power of the line, expressing the squared power with the active and reactive power phasors.

It is essential to introduce operational limits to the network to guarantee that it will be operating in a safe zone. Hence the intensity will be constrained as in (4.18), and the voltage must be between the interval defined in (4.19).

$$l_{ijt} \leq (I_{ij}^{mx})^2, \qquad \forall (i,j) \in \Omega\,; \quad \forall t \in T \tag{4.18}$$

$$(V_i^{mn})^2 \leq u_{it} \leq (V_i^{mx})^2, \qquad \forall i \in \Gamma\,; \quad \forall t \in T \tag{4.19}$$

The dispatchable power generation will use the model described in the previous chapters. Its limits are expressed in the following equations (4.20)-(4.23).

$$P_{it}^G \leq P_i^{Gmx} Y_{it}, \qquad \forall i \in \Gamma^{PQG}\,; \quad \forall t \in T \tag{4.20}$$

$$P_i^{Gmn} Y_{it} \leq P_{it}^G, \qquad \forall i \in \Gamma^{PQG}\,; \quad \forall t \in T \tag{4.21}$$

$$Q_{it}^G \leq Q_i^{Gmx} Y_{it}, \qquad \forall i \in \Gamma^{PQG}\,; \quad \forall t \in T \tag{4.22}$$

$$Q_i^{Gmn} Y_{it} \leq Q_{it}^G, \qquad \forall i \in \Gamma^{PQG}\,; \quad \forall t \in T \tag{4.23}$$

The batteries model previously developed is formulated in equations (4.24)-(4.27).

$$SoC\,(t=0) = SoC_i \tag{4.24}$$

$$SoC(t) = SoC(t-1) + \eta \, P_{it}^{b,char} \frac{\triangle t}{Cap^{bat}} - \frac{1}{\eta} \, P_{it}^{b,dischar} \frac{\triangle t}{Cap^{bat}}, \qquad \forall i \in \Gamma^{BAT}\,; \quad \forall t \in T \tag{4.25}$$

$$0 \leq P_{it}^{b,char} \leq M_{it} P_{mx}^b, \qquad \forall i \in \Gamma^{BAT}\,; \quad \forall t \in T \tag{4.26}$$

$$0 \leq P_{it}^{b,dischar} \leq (1 - M_{it}) P_{mx}^b, \qquad \forall i \in \Gamma^{BAT}\,; \quad \forall t \in T \tag{4.27}$$

Finally, the photovoltaic generation is added to the formulation, expressions (4.28)-(4.29). All the buses in the model that are not the slack one are considered as PQ unless there is solar generation. Every node with photovoltaic power stations will be considered PV buses.

$$P_{it}^{pv} \leq F_t^{pv} C_i, \qquad \forall i \in \Gamma^{PV}\,; \quad \forall t \in T \tag{4.28}$$

$$-0.35 P_{it}^{pv} \leq Q_{it}^{pv} \leq 0.4 P_{it}^{pv}, \qquad \forall i \in \Gamma^{PV}\,; \quad \forall t \in T \tag{4.29}$$

Because all the generation and the charge and discharge power of the batteries are considered to be aggregated, they are implemented to the power system in the net power consumption calculated at each node. This balance is done at each node and is computed as the power imports minus the power exports. This variable could be simplified in the equations by directly substituting the balance in the previous power balance. However, formulated as a separate variable allows to analyze each node balances better and is clearer to implement, expressions (4.30) and (4.31).

$$P_{it}^{net} = P_{it}^{C} - P_{it}^{g} + P_{it}^{b,char} - P_{it}^{b,dischar} - P_{it}^{pv}, \quad \forall i \in \Gamma \setminus \{1\}\,; \quad \forall t \in T \tag{4.30}$$

$$Q_{it}^{net} = Q_{it}^{C} - Q_{it}^{g} - Q_{it}^{pv}, \quad \forall i \in \Gamma \setminus \{1\}\,; \quad \forall t \in T \tag{4.31}$$

With the formulation above, the slack node must be treated as a particular case since it will not have any batteries, generation or demand. The only power present at the net power balance will be the entering from or exiting power to the external network. Therefore, the balance will be modelled as follows in equations (4.32)-(4.33).

The signs are expressly used so that when the network imports power, the variable P_{it}^{ext} is positive and when the network exports power, it is negative.

$$-P_{it}^{net} = -P_{it}^{ext}, \qquad \forall i \in \Gamma^{S}\,; \quad \forall t \in T \tag{4.32}$$

$$-Q_{it}^{net} = -Q_{it}^{ext}, \qquad \forall i \in \Gamma^{S}\,; \quad \forall t \in T \tag{4.33}$$

Objective function

The objective of the problem is to minimize the operation costs of a MVDN, intending to see how the use of different BESS and DRES parameters can affect the economic model of the power system.

With this purpose, the objective function is divided into four different terms, each representing a different type of operational cost of the system.

- Cost 1: Electricity trading with the external grid.

The following equation (4.34) models the economic relationship with the external grid, with established hourly electricity rates, which are the same for buying and selling. These electricity rates will be set in the next chapter based on the actual prices in Spain.

$$Cost1 = \sum_{i} \sum_{t} (P_{it}^{ext}\, ERates_t), \qquad \forall i \in \Gamma^S\,; \quad \forall t \in T \tag{4.34}$$

As stated before, when the network is importing current, the power variable will be positive. Thus the cost will increase at the electricity price. However, if the network is selling current to the external grid, the cost function will decrease with the same rates.

- Cost 2: Power Losses Cost.

Power loss minimization has two approaches, the slack bus approach and the summation of all losses in each line of the network. The first approach is implemented with the Cost1 equation and can be used in both linear and non-linear problems. This function already considers the power losses since all the energy dissipated in the lines is energy that the network will have to buy to the external grid. Consequently, if the DN aims to minimize the cost of buying electricity, it will reduce the power lost in the system. The main disadvantage of this method is that it can only minimize the total losses and not the losses on specific areas of the grid.

The second approach is introduced in this subsection, and its main advantage is that it allows the minimization of power losses in specific lines. This approach is also applied to give more relevance to the power dissipated in the system.

The price of the power losses in the distribution network is modelled with the following equation (4.35). The cost for MW lost is fixed throughout the day.

$$Cost2 = \sum_{(i,j)} \sum_{t} (r_{ij}\, l_{ijt}\, \rho^{losses}), \qquad \forall (i,j) \in \Omega\,; \quad \forall t \in T \tag{4.35}$$

- Cost 3: Dispatchable Generation Cost.

For the diesel generators, the model will use a quadratic cost function that approximates the actual cost function for this type of generation in a reliable way. The second-order polynomial consists of three terms. It is expressed as follows:

$$Cost3a = \sum_{i} \sum_{t} (a_g\, Y_{it} + b_g\, P_{it}^{G} + c_g\, P_{it}^{G2})\,, \qquad \forall i \in \Gamma^S\,; \quad \forall t \in T \tag{4.36}$$

The constant term requires the connection/disconnection binary variable to ensure that the fixed cost is not added if the generator is turned off.

Nonetheless, in the study cases the model will use a linear approximation of this function by defining a linear regression equation of the quadratic cost function. The linearization is needed to reduce the computation time of the problem, since the solver available for this thesis requires various hours to reach the optimal variables with the quadratic expression.

The ideal solution would be to acquire the license of a more potent solver, such as the IBM CPLEX, that works with non-linear models more efficiently. Nevertheless, these types of solvers are very expensive, and was not available during the realization of this project.

In conclusion, the equation used in the case studies will be expressed as in the equivalence (4.37), where a_{gr} and b_{gr} are the regression coefficients of the quadratic diesel cost function.

$$Cost3b = \sum_{i} \sum_{t} (a_{gr}\, Y_{it} + b_{gr}\, P_{it}^{G})\,, \qquad \forall i \in \Gamma^{S}\,; \quad \forall t \in T \tag{4.37}$$

- Cost 4: Photovoltaic Curtailment Cost.

Solar curtailment implies that solar power which could be produced remains unused because the power system cannot accommodate more energy. In general, the curtailment of any DRES goes against European directives and national laws. The European Commission introduced this policy in the past decade to enhance and prioritize renewable production before any other type of generation in the distribution grids. When this happens, the DSO are required to pay a penalty for every kWh that could have been used. For example, in 2016, Spain curtailed a total of 113 GWh from renewable sources, which implied 675.000 euros in compensation payments to the DRES operators. [Swa17] [Eur18]

This thesis will fix a cost for each kWh curtailed by the power system, represented with the following equation (4.38).

$$Cost4 = \sum_{i} \sum_{t} [(F_{t}^{pv}\, C_{i} - P_{it}^{pv})\rho^{curtailment}] \qquad \forall i \in \Gamma^{PV}\,; \quad \forall t \in T \tag{4.38}$$

The operating cost of the power system considered in the optimization problem will be the sum of the four costs expressed in this section, as in equation (4.39).

$$Op.Cost = cost1 + cost2 + cost3b + cost4 \tag{4.39}$$

Developing the costs, the objective function is expressed in the equation (4.40).

$$min \sum_{i}\sum_{t}[((F_t^{pv}\, C_i - P_{it}^{pv})\rho^{curtailment}) + (a_g\, Y_{it} + b_g\, P_{it}^{G} + c_g\, P_{it}^{G2}) + (P_{it}^{ext}\, ERates_t)] + \sum_{(i,j)}\sum_{t}(r_{ij}\, l_{ijt}\, \rho^{losses}) \qquad \forall i \in \Gamma\,; \forall (i,j) \in \Omega\,; \quad \forall t \in T \tag{4.40}$$

4.2 Optimal Power Flow Relaxation

The previous chapters emphasized the importance of the convexity of the model in finding a global optimum for the algorithm.

To achieve this, the model will apply the second-order cone relaxation in the equation (4.17), which represents the outline of one of these types of cone. Relaxing the equality of the formula, the feasible points can be anywhere but outside the cone, thereby the equation (4.41) will be convex.

$$l_{ijt} \geq \frac{P_{ijt}^2 + Q_{ijt}^2}{u_{it}}, \qquad \forall (i,j) \in \Omega \quad \forall t \in T \tag{4.41}$$

Bearing in mind that the solution must have physical sense, the equality always has to be satisfied. Thereby the results will require a meticulous analysis in the post-processing to make sure that the apparent flow of the line equality expressed in (4.17) is fulfilled.

Furthermore, towards formulating the equation in the GAMS solver, the equality needs to be developed. This is because the GAMS software works better if there are not any quotients. Therefore, the following equation (4.42) will be the second-order cone set of constraints used in the model.

$$(2P_{ijt})^2 + (2Q_{ijt})^2 + (l_{ijt} - u_{it})^2 - (l_{ijt} + u_{it})^2 \leq 0, \qquad \forall (i,j) \in \Omega \quad \forall t \in T \tag{4.42}$$

This last equation comes from a quick manipulation of the terms towards obtaining remarkable identities of the current and voltage instead of their multiplication. The development of the formula is shown below with expressions (4.43)-(4.46).

$$l_{ijt} u_{it} \geq P_{ijt}^2 + Q_{ijt}^2, \qquad \forall (i,j) \in \Omega \quad \forall t \in T \tag{4.43}$$

$$4 l_{ijt} u_{it} \geq 4P_{ijt}^2 + 4Q_{ijt}^2, \qquad \forall (i,j) \in \Omega \quad \forall t \in T \tag{4.44}$$

$$2 l_{ijt} u_{it} + 2 l_{ijt} u_{it} + l_{ijt}^2 - l_{ijt}^2 + u_{it}^2 - u_{it}^2 \geq 4P_{ijt}^2 + 4Q_{ijt}^2, \qquad \forall (i,j) \in \Omega \quad \forall t \in T \tag{4.45}$$

$$(l_{ijt} - u_{it})^2 - (l_{ijt} + u_{it})^2 \geq (2P_{ijt}^2) + (2Q_{ijt})^2, \qquad \forall (i,j) \in \Omega \quad \forall t \in T \tag{4.46}$$

When the optimal solution is feasible to the non-relaxed problem, the relaxation is said to be exact. The problem's solution must be exact because otherwise the solution will not be satisfying the power flow equations or the inequality constraints which would not make any physical sense.

This second-order cone relaxation is studied in detail in [FL12]. In that article, the authors demonstrate that this relaxation is exact if the following conditions are met:

- The network graph is connected.
- The objective function is convex.
- The objective function of the problem is strictly increasing in current, non increasing in load, and independent of the apparent power.
- The optimal power flow problem is feasible.

Because the model does not follow all the aforementioned conditions, it cannot guarantee that the solution will be feasible to the non-relaxed problem. So the model will require to verify if the solution is exact or not and develop some strategies to find the exact optimal solution if it is not exact.

To check if the solution is exact, the model will use a new parameter for the post-processing. This parameter will be initialized with a value of 1 and will go through all the system lines at every period checking if the apparent power flow of a line equality is met. If there were any line where the equation is not fulfilled, then the parameter would be set at 0 and the solution would not be feasible. This algorithm will be formulated as in the succeeding expression.

$$exactness = 1$$
$$if\ (2P_{ijt})^2 + (2Q_{ijt})^2 + (l_{ijt} - u_{it})^2 - (l_{ijt} + u_{it})^2 \leq -\xi : \qquad \forall (i,j) \in \Omega \quad \forall t \in T$$
$$exactness = 0$$

Note that an absolute zero is not needed to fulfil the condition but a very small threshold. The reason being that the optimization software does not work with round zeros since its numerical accuracy is not perfect. Therefore, the solver will consider the solution to be exact when all the residuals are so close to zero that can be neglected, more concretely, below 1e-3 p.u.

4.3 Model implementation

In order to solve the OPF, all the formulations must be adapted to an optimization solver. This thesis uses a specific software for mathematical optimization called GAMS that supports non-linear, linear, and mixed-integer problems choosing between an extensive list of powerful embedded solvers. This software uses a math programming language different from the numerical analysis language, as in MATLAB, which enables a more concise algebraic formulation. The main advantage of this program is that it allows the user to build the algorithm incrementally and change its statements easily.

The major disadvantages of this environment appear when working with large models. The parameters definitions become really slow and tiresome, and the solution report becomes indecipherable and too much to chew with its tools. Also, the post-processing in GAMS is very basic; thus, it is very difficult to analyze the results properly.

Nevertheless, these two drawbacks of the software can be solved with GDXMRW (GDX-Matlab Read/Write). It is a suite of utilities that allows the user to interface GAMS and MATLAB already included in the GAMS distribution. This tool allows to define the model parameters easily in MATLAB, export them to a .gdx file which GAMS can interpret and use to solve the problem. Then the optimization solver returns another .gdx file that contains the optimization results which MATLAB reinterprets. Also, Microsoft Excel is used to define certain parameters and to plot some results. Figure 5 represents a schematic of the process just defined.

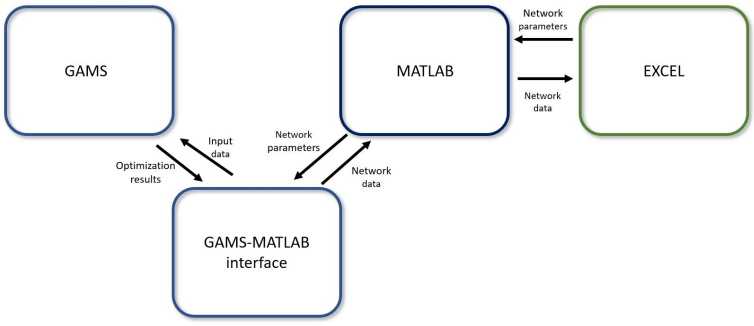

Figure 5: Interfacing of MATLAB-GAMS-EXCEL environments. (Own development)

5 Optimal Power Flow Application

5.1 Case Study Parameters

This section will apply and analyze the formulation developed in previous chapters to a radial distribution system from the IEEE test networks collection.

A simplified design of the network is represented in Figure 6. The study of the behaviour of the distribution network will integrate four models: dispatchable and non-dispatchable generation, loads, and battery energy storage systems.

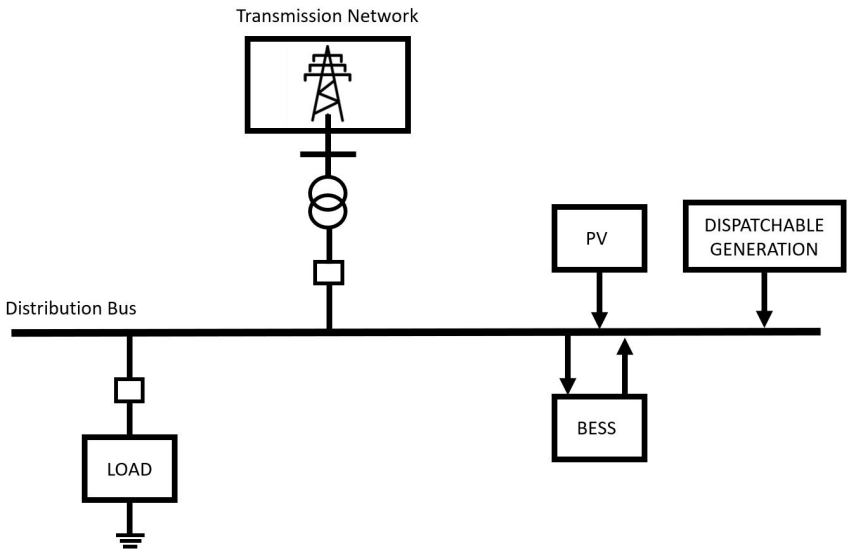

Figure 6: Simplified design of the distribution system. Based on [AAK20]

5.1.1 Network Parameters

The chosen network in the present study is based on the IEEE 33 which consist of 33 buses and 32 lines. The standard bus system is represented in Figure 7. As can be seen in the representation, it has been assumed that all the nodes have loads except the slack one.

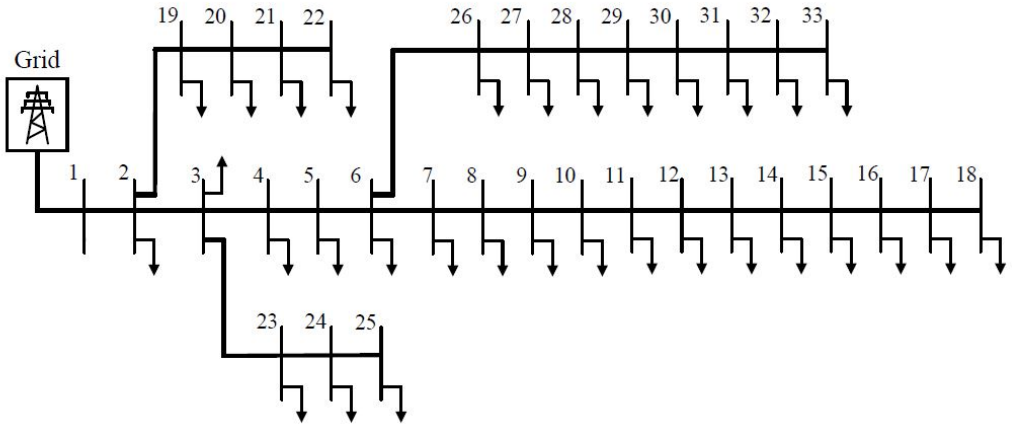

Figure 7: IEEE 33-Bus Distribution System. Based on [AAK20]

As previously stated, all the calculations in this model will be made in a per-unit system. Working with normalized variables reduces the computation complexity, simplifies the evaluation and makes the system's characteristics more comprehensible. The base values used for this power system are represented in Table 6. [Mom09]

Parameter	Value	Units
S_{base}	1.000	kVA
V_{base}	12,66	kV
Z_{base}	$V_{base}^2/S_{base} = 160,276$	Ω
I_{base}	$V_{base}/(\sqrt{3}\,Z_{base}) = 45,604$	A

Table 6: Base Values for the per-unit system

The branch characteristics of the network are defined in Table 7. The branch type is not specified because all the lines are defined as the same class. Also, the voltage limits at each node are between 1,1 p.u. and 0,9 p.u.

From Bus	To Bus	R[p.u.]	X[p.u.]	Imx[p.u.]
1	2	0,0922/Z_{base}	0,0470/Z_{base}	22
2	3	0,4930/Z_{base}	0,2511/Z_{base}	22
3	4	0,3660/Z_{base}	0,1864/Z_{base}	22
4	5	0,3811/Z_{base}	0,1941/Z_{base}	22
5	6	0,8190/Z_{base}	0,7070/Z_{base}	22
6	7	0,1872/Z_{base}	0,6188/Z_{base}	22
7	8	0,7114/Z_{base}	0,2351/Z_{base}	22
8	9	1,0300/Z_{base}	0,7400/Z_{base}	22
9	10	1,0440/Z_{base}	0,7400/Z_{base}	22
10	11	0,1966/Z_{base}	0,0650/Z_{base}	22
11	12	0,3744/Z_{base}	0,1238/Z_{base}	22
12	13	1,4680/Z_{base}	1,1550/Z_{base}	22
13	14	0,5416/Z_{base}	0,7129/Z_{base}	22
14	15	0,5910/Z_{base}	0,5260/Z_{base}	22
15	16	0,7463/Z_{base}	0,5450/Z_{base}	22
16	17	1,2890/Z_{base}	1,7210/Z_{base}	22
17	18	0,7320/Z_{base}	0,5740/Z_{base}	22
2	19	0,1640/Z_{base}	0,1565/Z_{base}	22
19	20	1,5042/Z_{base}	1,3554/Z_{base}	22
20	21	0,4095/Z_{base}	0,4784/Z_{base}	22
21	22	0,7089/Z_{base}	0,9373/Z_{base}	22
3	23	0,4512/Z_{base}	0,3083/Z_{base}	22
23	24	0,8980/Z_{base}	0,7091/Z_{base}	22
24	25	0,8960/Z_{base}	0,7011/Z_{base}	22
6	26	0,2030/Z_{base}	0,1034/Z_{base}	22
26	27	0,2842/Z_{base}	0,1447/Z_{base}	22
27	28	1,0590/Z_{base}	0,9337/Z_{base}	22
28	29	0,8042/Z_{base}	0,7006/Z_{base}	22
29	30	0,5075/Z_{base}	0,2585/Z_{base}	22
30	31	0,9744/Z_{base}	0,9630/Z_{base}	22
31	32	0,3105/Z_{base}	0,3619/Z_{base}	22
32	33	0,3410/Z_{base}	0,5302/Z_{base}	22

Table 7: Branch characteristics of the network

5.1.2 Demand Modelling

The demand of each bus throughout the day is modelled with five base profiles. These are based on an article published by Cigré in 2013. [Cig14] The model will extrapolate two different profiles for residential use and three different profiles for commercial/industrial use. Then the demand at each node will be calculated as the combination of a residential and an industrial profile.

In the following list, the weights used to calculate the profiles are presented. The first percentage represents the percentage of commercial/industrial power use in the bus and the second one residential power use.

- 12 buses with 50/50 %
- 6 nodes with 60/40 %
- 6 nodes with 40/60 %
- 4 nodes with 70/30 %
- 4 nodes with 30/70 %

Combining these five types of weightings with the five profiles available results in 26 different load profiles, so almost any bus in the system has a different load profile than the others.

The following Figure 8 shows the five base profiles used to make each bus profile.

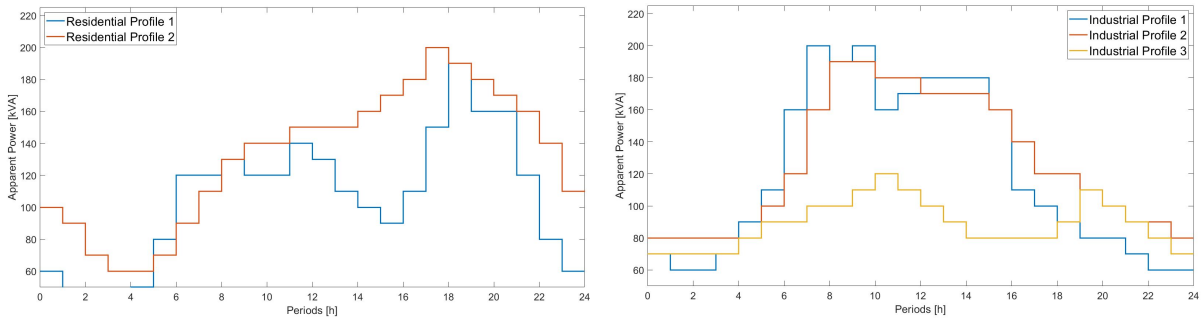

(a) Residential Load Profiles (b) Industrial/Commercial Load Profiles

Figure 8: Base Load Profiles

Figures 9 and 10 show the active and reactive power of the 26 different profiles that model the demand in the network.

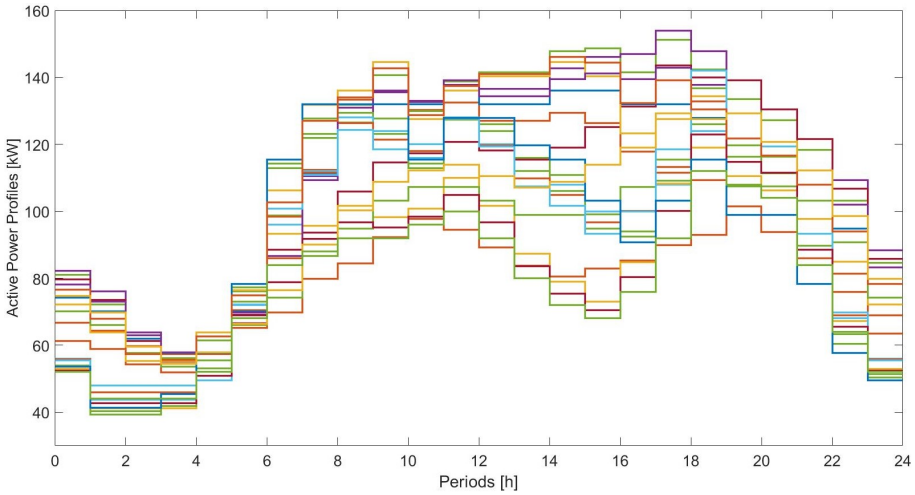

Figure 9: Active Power Profiles

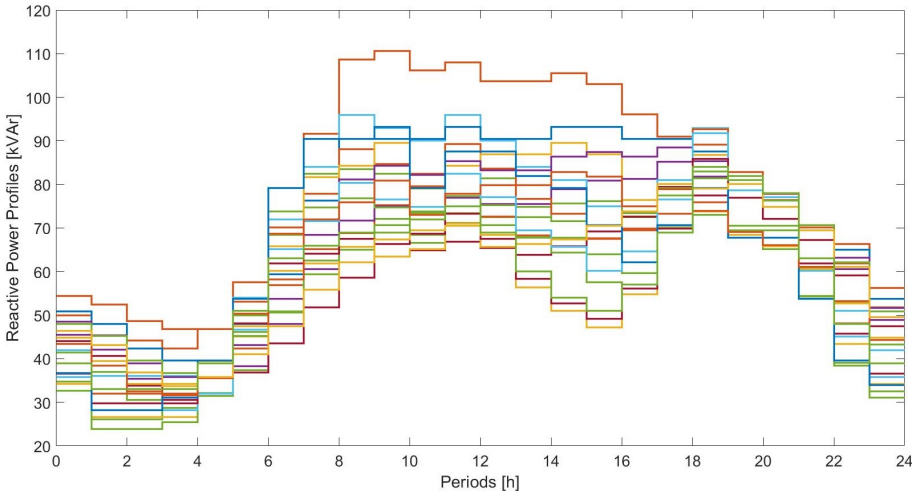

Figure 10: Reactive Power Profiles

The overall power demand of the whole network is expressed in Table 8, which plots the active and reactive power demand of each node in p.u. for the whole day. The slack bus does not appear since it does not have power consumption.

Bus	Active Power	Reactive Power	Power Factor	Bus	Active Power	Reactive Power	Power Factor
2	2,386	1,945	0,775	18	2,237	1,561	0,82
3	2,241	1,448	0,84	19	2,249	1,365	0,855
4	2,341	1,451	0,85	20	2,232	1,528	0,825
5	2,747	1,407	0,89	21	2,650	1,643	0,85
6	2,661	1,508	0,87	22	2,562	1,755	0,825
7	2,562	1,755	0,825	23	2,237	1,561	0,82
8	2,224	1,668	0,8	24	2,576	1,596	0,85
9	1,893	1,543	0,775	25	2,650	1,643	0,85
10	2,576	1,596	0,85	26	2,186	1,498	0,825
11	2,74	1,516	0,875	27	2,248	1,452	0,84
12	2,241	1,448	0,84	28	1,939	1,353	0,82
13	2,224	1,668	0,8	29	2,232	1,529	0,825
14	2,501	1,384	0,875	30	2,661	1,508	0,87
15	1,935	1,353	0,82	31	2,341	1,451	0,85
16	2,186	1,498	0,825	32	1,86	1,395	0,8
17	2,018	1,304	0,84	33	1,86	1,395	0,8

Table 8: Power Demand at each bus in p.u.

The total power consumption of the system throughout the day is 74,196 kW and 48,723 kVAr. This power demand data will remain constant in all the study cases of this thesis.

5.1.3 Dispatchable Generation Parameters

As previously stated in the formulation section, the model will consider a second-order polynomial as the diesel generation cost function. This one is based on the formulation proposed in [Ahn+13] and it is expressed in Table 9.

a_g [€]	b_g [€/kW]	c_g [€/$(kW)^2$]
14,53	8,3e-2	1e-4

Table 9: Diesel generation cost function parameters

However, in order to linearize the objective function of the problem, the economic model will use an approximation of this function. Linear regression in the generation interval of the system will be used.

The diesel generation data is presented in Table 10. It consists of seven diesel generators distributed over the entire network with a maximum power generation of 1.660 kW/h or 39.840 kW/day.

Bus	P_{Gmax} $[kW]$	P_{Gmin} $[kW]$	Q_{Gmax} $[kW]$	Q_{Gmin} $[kW]$
2	600	180	300	-300
6	320	96	160	-160
11	80	24	40	-40
17	100	30	50	-50
21	160	48	80	-80
26	280	84	140	-140
29	120	36	60	-60

Table 10: Generation data

Assuming the same cost function for the seven generators of the system, the regression function will be calculated in the interval between the maximum and the minimum generation of a single bus of all the study cases.

As can be seen in Figure 11, the linear regression correctly approximates the quadratic function in the power generation interval needed. The R^2 of a 0,9916 is an excellent indicator that the regression is suitable.

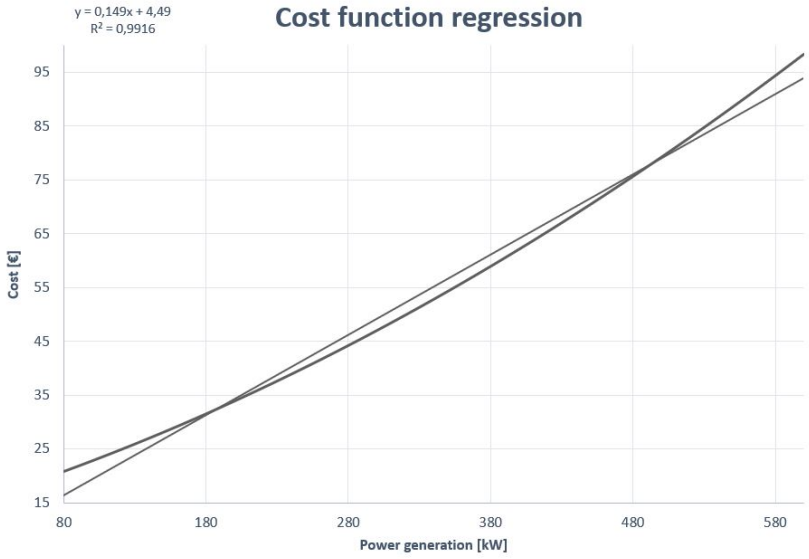

Figure 11: Cost function regression

To be sure that this model will not significantly alter the problem results, Figure 12 shows the relative error of the two functions. As illustrated, the error is almost always below the 5 % mark. Only at low power the relative error reaches higher percentages but this is due to the low operating cost at that level. A 20 % difference at that level would be 3€, which will not assume as significant.

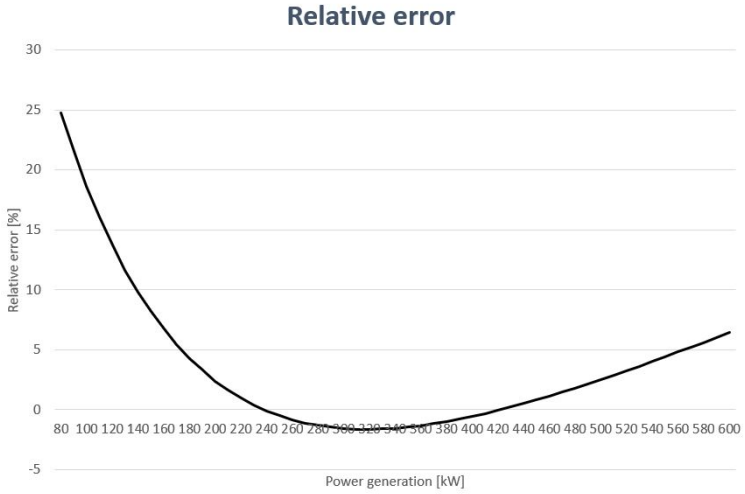

Figure 12: Relative error between the regression and the quadratic function

So the final parameters of the cost function are expressed in Table 11.

a_g [€]	b_g [€/kW]
4,49	0,149

Table 11: Linear diesel generation cost function parameters

In conclusion, although using a non-linear objective function would be the most accurate model, due to software limitations and computational time reduction, the linear approximation of the generation cost function will be assumed as correct.

5.1.4 Photovoltaic Generation Parameters

Defining the photovoltaic generation model requires two parameters, the solar forecast of the day and the rated power of the solar power plant.

The solar forecast is based on the model used in [CZ17] representing the power available on a sunny day in the summer and it is presented in the following Figure 13. The profile employs

a per-unit system that uses the rated energy capacity of the batteries as the base value.

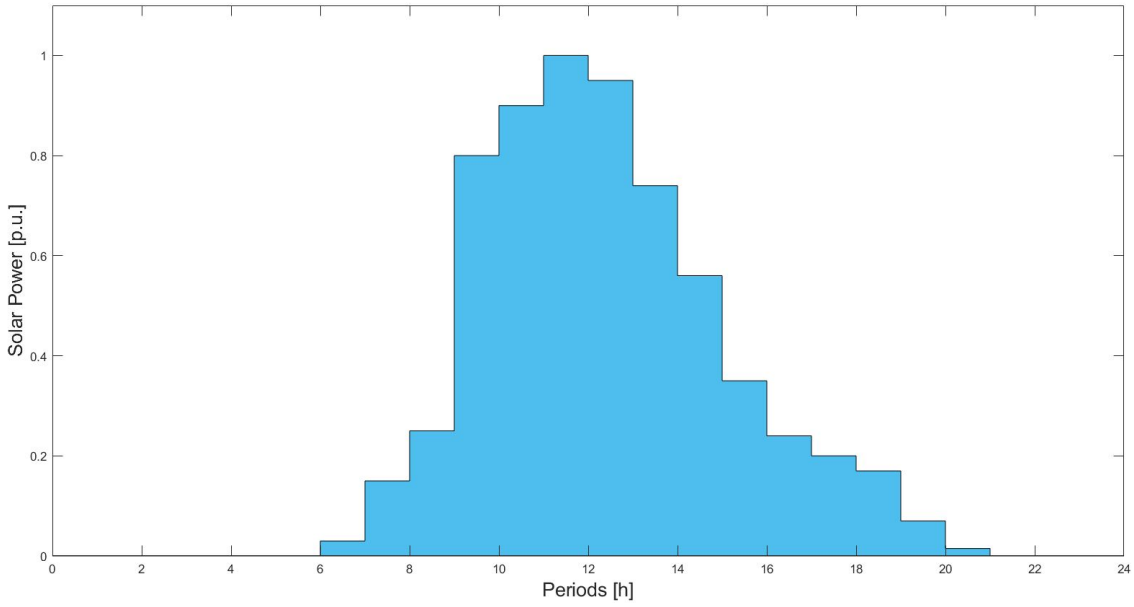

Figure 13: Solar Power Forecast

The rated power of the six photovoltaic plants in the system will vary depending on the study case. In the first case, the solar and the dispatchable power capabilities are very equal, and in the other cases, there is an excess of solar energy generation compared to the system's demand. These scenarios will be defined at the beginning of each study.

5.1.5 Batteries parameters

The model of the six batteries that are placed in the distribution network requires the specification of various parameters: the initial state of charge, the efficiency, the rated energy capacity and the maximum and minimum power at which it can be charged or discharged. This thesis will assume that all the batteries present the same characteristics, with the specifications indicated in Table 12. [Clo+19]

$SoCi$	Cap^{bat} $[kW/h]$	P^{b}_{mx} [p.u.]	η
0,25	4.480	2,2	0,9

Table 12: Battery Parameters

As expressed in the formulation, the problem will assume that the charging and discharging efficiencies are equal and that the maximum charge and discharge power are the same.

The sizing of the batteries is a very interesting topic that can be investigated in future work of the thesis. There are a lot of algorithms and strategies to find the optimal battery parameters that improve the system's performance while minimizing the costs associated with the batteries, such as the battery cost, the installation cost, and the maintenance cost. It has been widely studied in recent years, normally also considering the battery placement altogether. Articles like [SG20] and [Boo+20] propose algorithms to properly size and locate the BESS.

This simulation though, due to time constraints, it will not consider this optimization. The location used is based on a battery optimal placement article explained in the next chapter 5.1.7. The battery parameters are summarized in the previous Table 12, and they apply to the six batteries used. The total capacity is enough to store almost 25 % of the solar generation of the study case and the maximum charging and discharging power are 2.200 kW.

It is important to add that while the operation planning starts with the batteries 25 % charged, no condition for its state of charge is imposed in the final period. Ergo, the level at which the batteries are charged at the ending will only depend on the optimal operation variables of that day. It could either be that a battery is fully charged at the end or that it does not have any energy stored left. This is to allow more freedom for the model to find the best conditions.

To find the optimal state of charge of each battery on the final period of the day, a more extensive study should be done considering the system previsions and forecasts for the following days.

5.1.6 Electricity Rates

In the following Table 13 is illustrated the hourly electricity rates used in the study cases. Those are based on the electricity prices in Spain during the year 2020.

Period	€/kWh	Period	€/kWh
1	147,59	13	138,99
2	144,51	14	137,35
3	144,35	15	133,11
4	147,32	16	131,6
5	145,83	17	128,55
6	150,89	18	129,49
7	150,37	19	134,91
8	152,07	20	143,12
9	151,18	21	150,6
10	147,48	22	153,48
11	140,45	23	152,89
12	139,06	24	152,68

Table 13: Hourly Electricity Rates

5.1.7 Network topology

The topology of the network is a highly complex aspect of network planning. The location of the generators, the solar power plants, and the batteries can make a big difference in the network behaviour. In these study cases, the nodes and links of the network are already defined by the chosen network of the IEEE repertoire. However, the placement of the diesel generators, the photovoltaic panels and the batteries depends on the scenario and its objective.

The diesel generators will be placed on nodes 2, 6, 11, 17, 21, 26, and 29 to recreate the topography in the thesis [Mas18].

The optimal placement of BESS is essential in network planning to maximize the system performance and reduce economic costs, particularly in DN. The formulation of an optimal BESS placement model that is coherent and effectively feasible is a very complicated issue, especially for large-scale systems. [AES15]. Nevertheless, as the applications of batteries in power system increases, numerous propositions for techno-economic sizing and sitting of these devices have been recently published.

In [AAK20], the authors propose a GA to find the optimal allocation of the BESS to reduce overall power losses, also using the IEEE 33 network to test the strategy and comparing the

losses between different configurations.

The BESS and DRES will be placed emulating the previous article [AAK20]. In this paper, the authors arbitrarily install six solar PVs on the IEEE 33 MVDN and use a Genetic Algorithm optimization technique to optimally allocate six batteries in order to reduce power losses.

The final configuration proposed by the researchers and used in the case studies is the following. The solar panels are installed on nodes 3, 8, 14, 25, 30, and 31, and the batteries are installed on buses 8, 14, 24, 25, 30, and 31.

It is important to note that allocating the solar panels and the batteries in the same nodes as in that article is not guaranteed the best configuration in this scenario. Firstly, because the bus data and the generation data are different between the two studies. Secondly, although the power loss function is included in the objective function of the model, it also has three more functions. Ergo it cannot be said that the distribution assigned is optimal to the studied case.

However, it has been considered that a BESS and DRES placement that minimizes the power losses is a good strategy for the system since they are highly considered in the objective function. Network planning is a very challenging problem that will not be addressed in this thesis and that it is left for possible future work.

The scheme of the IEEE 33-Bus with dispatchable generation (G), solar generators (PV) and batteries (BESS) is represented in Figure 14.

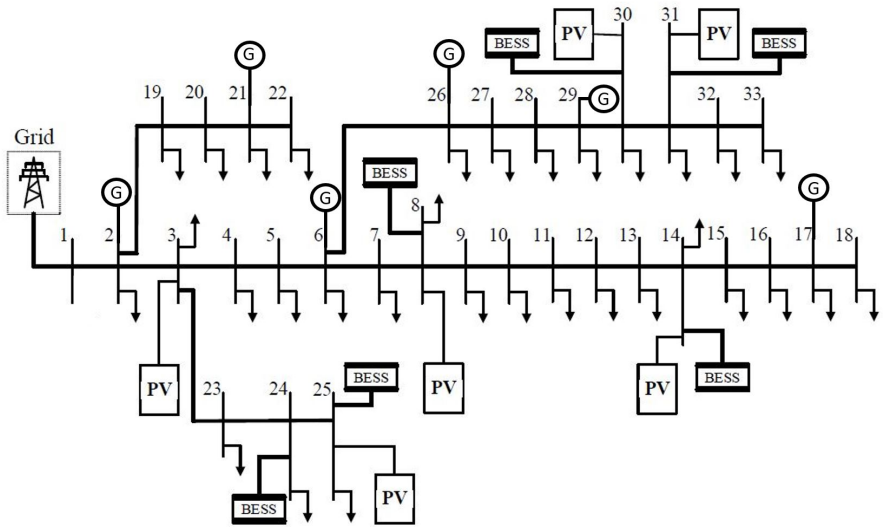

Figure 14: IEEE 33-Bus with diesel generation, DRES and BESS. Based on [AAK20]

Finally, it is important to remark that the model does not limit the amount of power exported or imported on the slack bus in the distribution network. This fact can be seen in the formulation as there is no limitation in the slack bus power balance. The system can sell electricity to the external grid if it has over generation and can buy power if the generators cannot cover its demand.

5.2 Results

This section will test and validate the optimal power flow with the IEEE 33-Bus network in three different scenarios. The first one will consider solar power production and dispatchable generation with both the same production capability. The second one will have more power generation capability than demand, and the third one will implement the six energy storage systems and see how it improves the model.

5.2.1 Case Study 1

The first study presents a standard scenario where the maximum energy that can be produced during a day with diesel generators is similar to the maximum that can be produced with solar panels. The system should not be dependant on the external grid to supply its demand. The total network generation can reach up to 81,089 MWh and the systems' demand throughout the day is 74,196 MWh, as is shown in Table 14.

Diesel	PV	Diesel+PV	Demand
39,84	41,249	81,089	74,196

Table 14: Energy Generation and Consumption of the system in MWh

However, because the solar panels only provide power during a limited time of the day, and in this case, no energy storage devices are considered, the system will be dependant on external power production. This can be seen in Figure 15, which represents the evolution of the power generation and the networks' demand. On the one hand, during the hours that there is no solar production, the system will require external energy to fulfil its consumption. On the other hand, during the peak hours of PV generation, more power can be generated than the systems' demand. In these hours, the network operation will determine if it is better to curtail power or generate in excess to sell the surplus energy to the external grid based on the objective function. Curtailing solar power is expensive, but also increasing the generators' output can lead to higher

power losses which are also expensive.

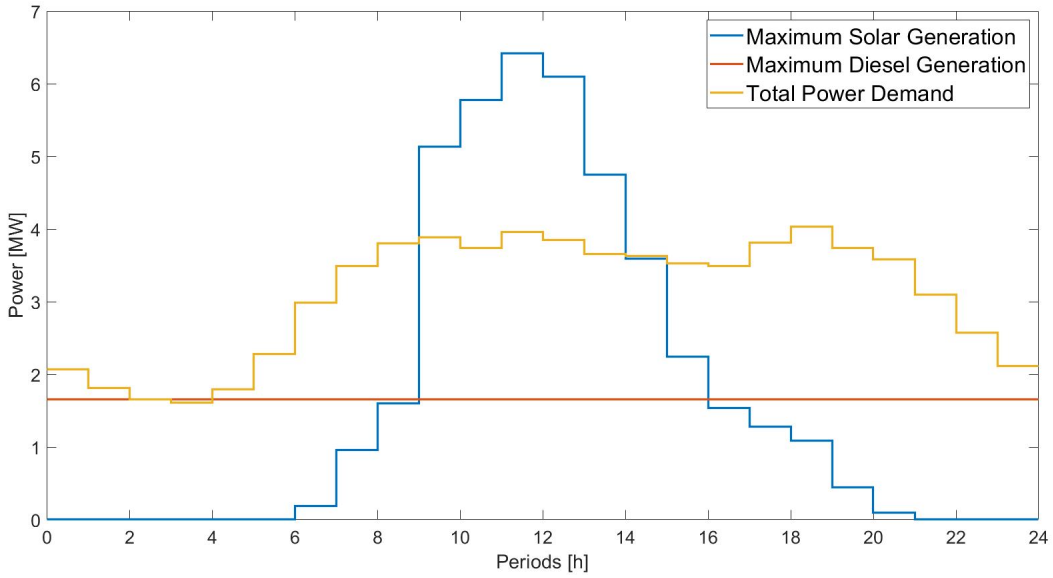

Figure 15: Maximum system's generation and demand

The solver used for this study in GAMS is the SCIP, which is especially effective for mixed integer programming (MIP) and mixed-integer non-linear programming (MINLP). The model consists of 8.017 variables and 10.632 equations. The solution provided by GAMS is exact, so the optimal solution is feasible to the non-relaxed problem. This means that all the system's lines satisfy the equation (5.1).

$$l_{ijt} = \frac{P_{ijt}^2 + Q_{ijt}^2}{u_{it}}, \qquad \forall (i,j) \in \Omega \quad \forall t \in T \tag{5.1}$$

The system's generation output can be seen in Figure 16. When there is no solar energy available, the network relies on the diesel generators to satisfy its demand. If the dispatchable power then is not enough, the remaining energy comes from the external grid. However, when the PV panels start to work, the solar power takes all over the network, producing more than the loads' needs. Also when this happens, the diesel generators are not turned off because the cost of producing energy at that moment is lower than the revenue that the system could get for that energy, even including the extra power losses.

As expected, the network does not curtail any solar power. The reasons being that solar power does not pose any direct cost to the operation, curtailment is expensive, and selling electricity to the grid is possible. If the power exchange were not possible, then curtailment would have been the only option.

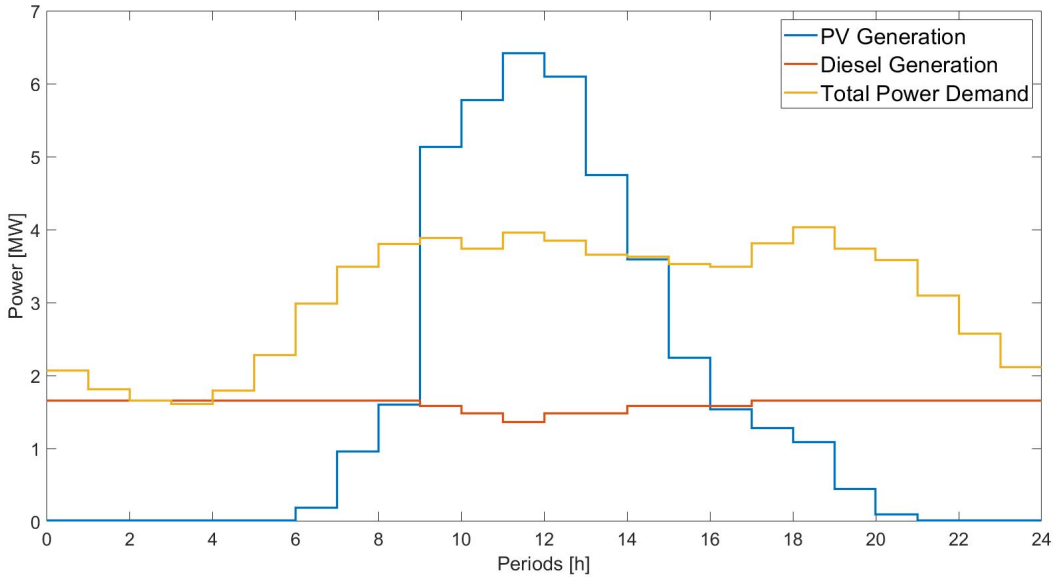

Figure 16: PV and Diesel generation/Demand in Case Study 1

A few things to remark about the results expressed in Figure 16. Because the network is connected to the grid, all the power generators can be running at their maximum stationary capability, since the excess of power from the loads can be sold. If there were not this possibility, the remaining power would have to be curtailed not to saturate the system.

Thereby having the possibility of exchanging power to the grid is an excellent alternative to energy storage devices, given that no solar production is curtailed. This renewable energy could be sent to networks with no solar resources. Of course, this only applies to the PV power, since the diesel generators can be easily turned off with no operational cost.

In Figure 17 can be seen more clearly this power exchange with the external grid in relation to the network generation. From sunrise to sunset, there is more electricity production, so the power balance is negative in the slack node, and at night the balance is positive to fulfil the remaining power that the fuel generators cannot cover.

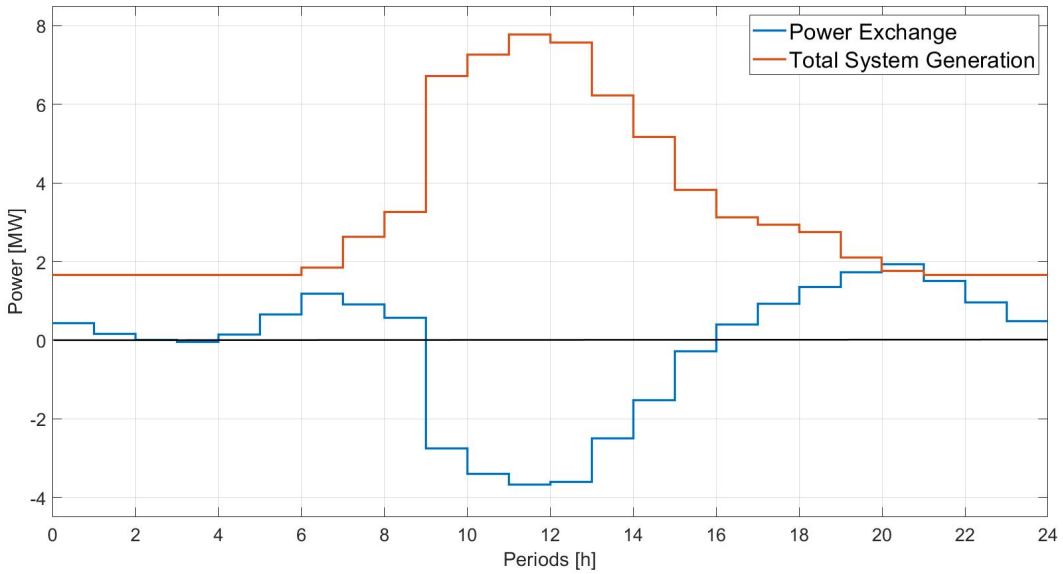

Figure 17: Total system's generation and power exchange in Case Study 1

These changes in the network consumption of electricity from the external grid entail differences in the network, for example, in the buses voltages. As it is known, the electrical intensity goes from high voltages to low voltages. Hence when the network is buying electricity from the external network, the buses' voltages will be lower than the reference voltage of the slack node. Moreover, when is selling power the buses voltages will be higher than the reference voltage of the slack node. This behaviour can be seen in Figure 18, where every colour represents a profile of one of the 33 nodes of the network.

In the time-frames when the system buys electricity, the voltages are below one p.u. However, when the solar panels are turned on, the network starts selling power and the voltages increase above the base one. The few potentials that are slightly below the reference in the peak hours are the most downstream nodes with no generation capacity, buses 19, 20, 21, and 22.

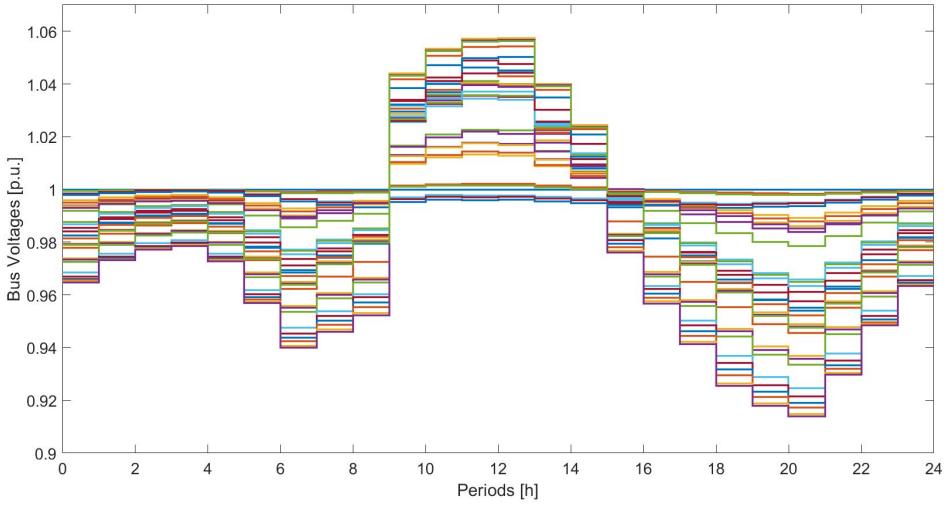

Figure 18: Buses Voltages Profiles throughout the day in p.u.

This also has an effect on the losses, which can be seen in the Figure 19. The power transmitted through a line is directly proportional to the voltage and the current intensity. Therefore these variations in the buses' voltages either reduce or increase the electrical current and consequently the losses. Hence, despite between 9 a.m. to 1 p.m. and 7 p.m. and 10 p.m. there is a big difference in the network's circulating power amount, the network losses are not significantly different. During the midday, the voltages are higher and the current is reduced, so fewer power losses to transport the same amount of power. Nevertheless, because the system imports much power at the end of the day, the voltages drop considerably, and the network needs more current to transport the same amount of energy, thus more power losses.

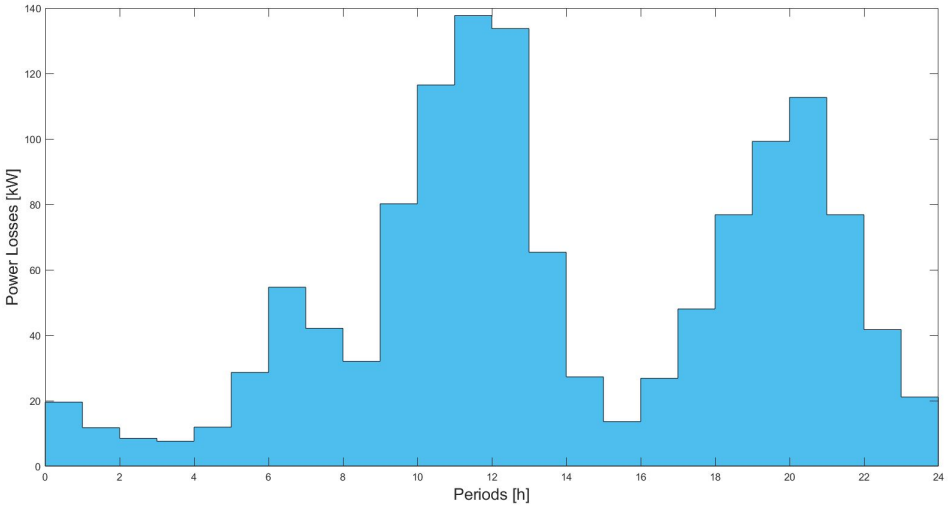

Figure 19: Total Power Losses throughout the day in p.u.

When the network is consuming energy from the external grid, the slack node has the highest voltage at one p.u. and the other buses reduce their voltage to be able to consume power. The lower the voltage, the more downstream is located the node. Nevertheless, when the network is selling electricity, the profiles are a little bit more complicated. The network still has to satisfy the demand at the same time that the current is generally going upstream. This is why not all voltage profiles are above the slack one. To see this more clearly, Figure 20 represents all the current directions.

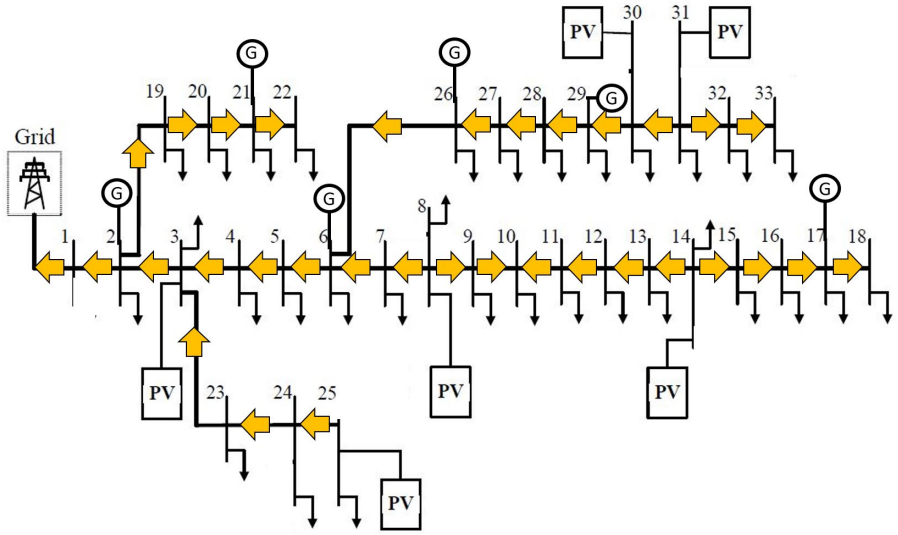

Figure 20: IEEE 33-Bus with the direction of the power flows. Based on [AAK20]

The following parameters are calculated to outline the network behaviour. $PGdiesel$ expresses the total system's dispatchable generation, $PGpv$ calculates the entire network's photovoltaic generation, and $PGslack$ computes the power exchange with the external grid of the day. Finally, PL determines the power losses on the network in a full-day operation. The expressions are formulated in (5.2), (5.3), (5.4), and (5.5).

$$PGdiesel = \sum_{i} \sum_{t} P_{it}^{G}\,, \qquad \forall i \in \Gamma^{PQG}\,; \quad \forall t \in T \tag{5.2}$$

$$PGpv = \sum_{i} \sum_{t} P_{it}^{pv}\,, \qquad \forall i \in \Gamma^{PV}\,; \quad \forall t \in T \tag{5.3}$$

$$PGslack = \sum_{i} \sum_{t} P_{it}^{G}\,, \qquad \forall i \in \Gamma^{S}\,; \quad \forall t \in T \tag{5.4}$$

$$PL = \sum_{(i,j)} \sum_{t} r_{ij}\, l_{ijt} \qquad \forall (i,j) \in \Omega\,; \quad \forall t \in T \tag{5.5}$$

To conclude this case study, Table 15 contains a summary of the network results.

Op. Cost[€]	I max [p.u.]	V max [p.u.]	V min [p.u.]
3,6466e+3	3,6817	1,0574	0,9139
	(From 2 to 1)	(Bus 31)	(Bus 18)
	(T = 12)	(T = 13)	(T = 21)
$PGdiesel$ [MWh]	$PGpv$ [MWh]	$PGslack$ [MWh]	PL [MWh]
38,68	41,249	-4,438	1,295

Table 15: Study Case Results

5.2.2 Case Study 2

The second case is motivated by the first one. The system's response to the peak PV energy poses the question of what would happen if the solar panels' rated power was higher. This is a very legitimate question because solar power is cost-free from an operational point of view, and adding more solar panels would mean that more electricity could be generated and sold to the grid. However, the system must operate in the physical constraints of the network all the time, thereby there will be a limit of energy produced before the network saturates.

So this study case will have the same distribution and parameter values as the previous one except the photovoltaic generators rated power, which will have now the capability to generate 178,5 % more than before. As it might be seen in Figure 21, the plot is the same as in the first simulation, Figure 15, but during the hours of sun, the maximum solar generation is much higher. This case will neither consider the BESS.

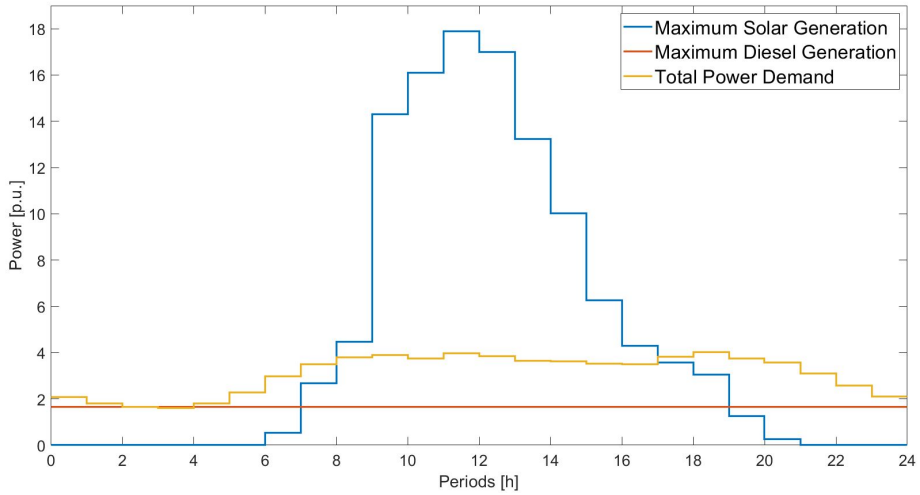

Figure 21: Generation and Consumption throughout the day in MWh

The case data is summarised in Table 16. Therefore in this simulation, the energy that can be produced doubles the energy that the loads require.

Diesel	PV	Diesel+PV	Demand
39,84	114,879	154,719	74,196

Table 16: Energy Generation and Consumption of the system in MWh

Again, the solver used for this study in GAMS is the SCIP. Because it only changed the batteries rated power, this model also consists of 8.017 variables and 10.632 equations. The solution provided by GAMS is optimal. However, the exactness parameter of the post-process is null, so the simulation is not exact. This means that the solver is finding a solution that is only possible when the relaxation is applied.

Although the apparent power balance of the lines is not satisfied during three periods only in the link from bus 16 to 17, it is a global problem. Meaning that it is not a singularity of that buses that the relaxation is not fulfilled, but a consequence of the whole network being flooded by power during the peak solar hours.

If the problem were not relaxed, the solver would find the generation limit and curtail the remaining energy that could not be produced. However, because the problem uses the second-order cone relaxation and the objective function wants to minimize the costs of cutting renewable power, the software finds another solution. In these circumstances, during the peak solar power production hours, instead of curtailing photovoltaic energy, it decides to increase this type of generation by virtually increasing electrical current to dissipate this surplus of energy in the form of power losses (rI^2).

The model justifies this strategy because the price of curtailing renewable energy is higher than dissipating it as power losses. Therefore, it virtually increases the current, increasing the power losses and not curtailing PV power. However, then the equality of the power balance (5.6) is not satisfied and the solution makes no physical sense. It would mean that the solution is on the interior of the second-order cone when it has to be on the surface.

$$l_{ijt} > \frac{P_{ijt}^2 + Q_{ijt}^2}{u_{it}}, \qquad \forall (i,j) \in \Omega \quad \forall t \in T \tag{5.6}$$

The reason behind why the model virtually increases the current in that particular line instead of in any other is an arduous task to understand. It would require a deep analysis of analyzing the mathematics and the theory behind the optimization technique. From an engineering perspective, it does not make much sense to commit resources to determine the reason. Instead, it is more intelligent to understand that the solution provided mathematically does not follow the laws of physics and try to find a strategy to obtain a viable solution.

Given that the model cannot guarantee that the relaxation will not fail in these types of problems, a solution recovery algorithm to find the global optimum of the non-relaxed problem, if the solution is not exact, is developed. This one will be based on the one proposed in [Swa17].

The main idea of this algorithm is to guarantee that the solution will be exact if there is a feasible solution. Thus the objective function needs to satisfy the conditions of section 4.2.

The problem's objective function is not strictly increasing in current. Hence the model requires a new objective function that satisfies this requirement. The most straightforward function that meets this condition is shown in (5.7).

$$\sum_{(i,j)} \sum_{t} r_{ij}\, l_{ijt} \quad \forall (i,j) \in \Omega\,; \quad \forall t \in T \tag{5.7}$$

Nevertheless, the goal of the model is to find the optimal variable values that minimize the operational cost and not the power losses. Consequently, the actual objective function will be considered in the new algorithm but as a constraint.

So the new problem will have the same 12.217 equations and 9.601 variables of the original one, but with the new objective function and with the added constraint of the desired objective function, expressed in (5.8). This parameter k will be updated every iteration to narrow down the desired objective function and find the minimum k value that satisfies the relaxation.

$$k \geq \sum_{i} \sum_{t} [((F_t^{pv}\, C_i - P_{it}^{pv})\rho^{curtailment}) + (a_g\, Y_{it} + b_g\, P_{it}^{G} + c_g\, P_{it}^{G2}) + (P_{it}^{ext}\, ERates_t)] + \sum_{(i,j)} \sum_{t} (r_{ij}\, l_{ijt}\, \rho^{losses}) \qquad \forall i \in \Gamma^{PV}\,; \forall (i,j) \in \Omega\,; \quad \forall t \in T \tag{5.8}$$

In the following algorithm, f^* will be the value of the desired objective function on the original model(M-PERIOD-SOCP) and f^{**} will be the value of the desired objective function on the new model(M-PERIOD-ALGOR).

The parameters High and Low are used to define the solution interval. Iter is used to count the iterations done in the simulation, and err is used to fix the maximum absolute error on the resulting solution. The initial k value has to be fixed into a higher number than the f^*. However, if it is too close to f^*, the algorithm may return an unfeasible solution, and if it is too high, it may increase the number of iterations to converge. It is difficult to fix a value for it, since every case is different and requires a bit of experience and trial and error.

Algorithm 1: Proposed algorithm

```
high=k
low = f*
k=(high+low)/2
iter=1
err = abs(high-low)
while err>5 do
    iter = iter+1
    solve M-PERIOD-ALGOR
    compute the exactness parameter
    if exactness=1 then
        High=f**
        k=(high+low)/2
        save results
    else
        low=k
        k=(high+low)/2
    end
    return results
end
```

The algorithm process is straightforward. If the solution of the model is not exact, it means that below that solution there is not any solution that holds the relaxation. Then the algorithm will limit the new model so that the objective function has to be bigger than that value. If the problem finds an exact solution, it will save the results, fix the solution as the high value, and try to find a better solution. This process will continue until the difference between the high and low parameters is lower than 5 €.

The high parameter will be updated with the objective value f^{**} so that it converges faster,

minimizing the number of iterations of the algorithm. Nevertheless, it is not the only way. Other approaches such as assigning k to the high value every time also work, as proposed in [Swa17], although they may require more iterations.

Figure 22 represents the iterative process of the proposed algorithm applied to the study case. The columns represent the desired objective value of the function. The high, low, and k parameters are recalculated in every iteration until they are almost equal. A red column means that the solution provided is not exact, and a blue column that it is exact.

It takes 11 iterations and 24 minutes to find the solution. Initially, the k value is significantly decreased until iteration 7 and 8, where the resulting k is lower than the optimal solution. Then the algorithm increases the lower bound until the k is higher than the optimal result. Then the k is slightly reduced until it converges to the optimal value. This final process can be seen more clearly in Figure 23.

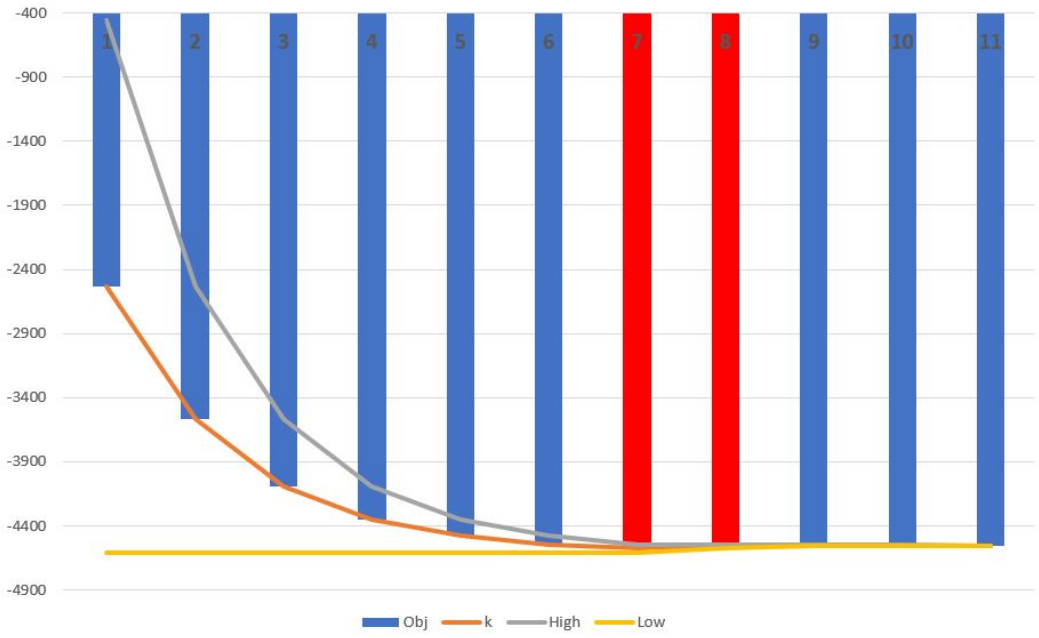

Figure 22: Iterative process of the algorithm

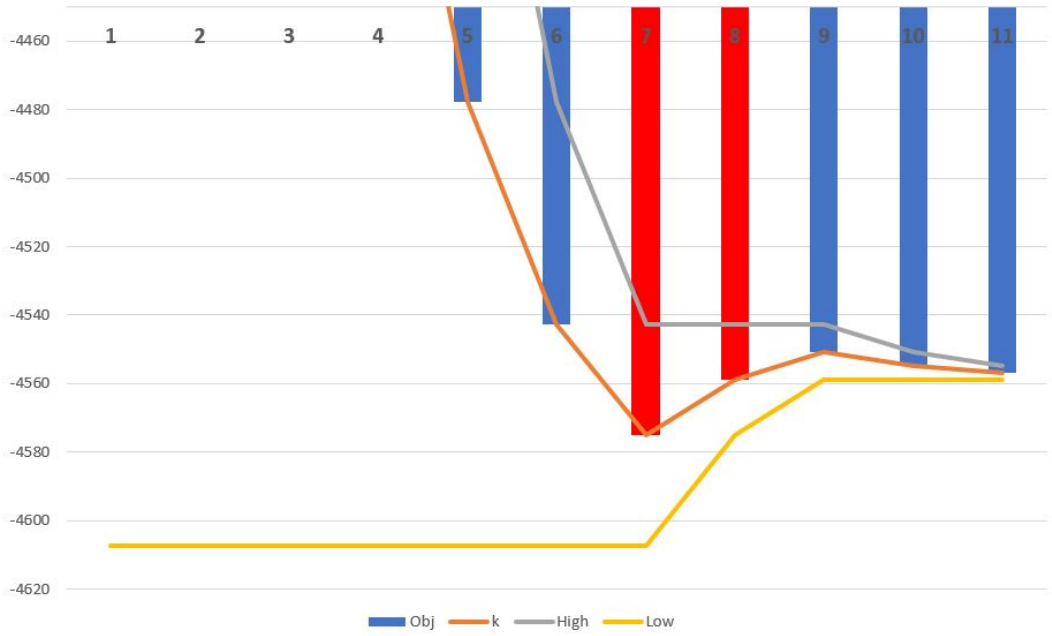

Figure 23: Final Iterative process of the algorithm

This algorithm applied to the previous case returns the optimal solution of the non-relaxed problem. Because the algorithm makes sure that the apparent power equation is fulfilled at all times, what the algorithm returns is the previous solution but instead of the network virtually increasing the power losses, curtailing power. Hence the solution presented next is very similar to the not exact one.

Comparing the exact and not exact results answers why the previous solution virtually increased the current. With the non-exact result, the operational cost of the network was -4.607,36 €, whereas with the exact solution is -4.556,74 €. So the optimization finds almost a 50€ difference between burning generated power and curtailing production. This leads to the conclusion that when the objective function is not strictly increasing in current, the operator must be very cautious with the second-order cone relaxation because the solver may find a not physically possible solution.

The exact solution has a similar behaviour with the previous case where the PV generation capability was lower. In this scenario, the hours before the solar production kicks in, it presents the same steady-state variables as before. It makes sense since the system's parameters are equal. The difference appears when the sun comes up. Then the system is pushed to the limit because of the enormous amount of power production capability.

The network's generation output can be seen in Figure 24. The solar power production is almost the same as the solar power profile, and that during the day there is more than 4,5 times more generation than demand. So the network's voltages and intensities will be configurated towards maximizing the power transmission towards the slack bus. The diesel generation is lower than in the previous case, but still, it is not turned off during the solar hours.

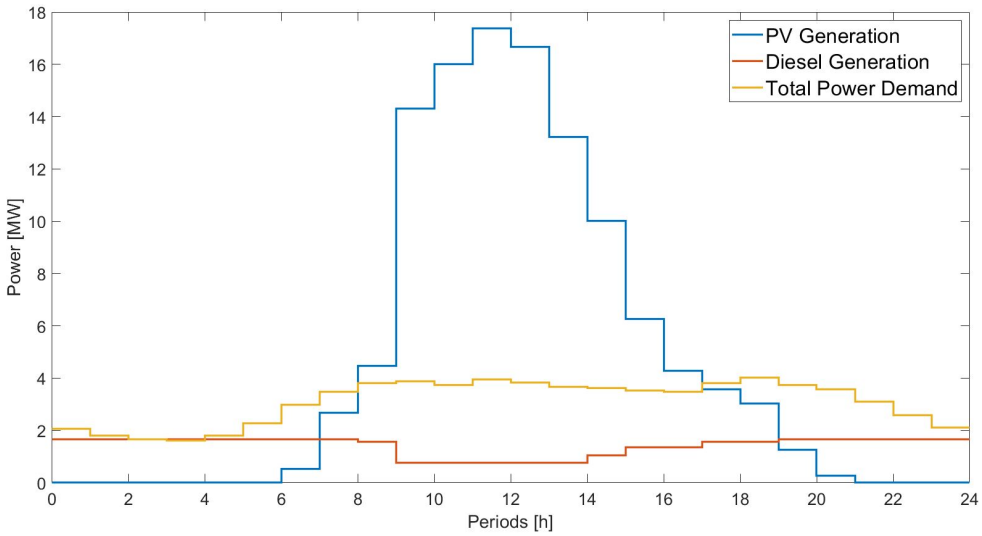

Figure 24: PV and Diesel Generation/Demand in Case Study 2

In Figure 25 can be seen the power exchange evolution during the day. As expected, during dark hours the power bought is equal to the case study 1. However, during sunny hours the power sold to the external grid is more than two times greater than previously.

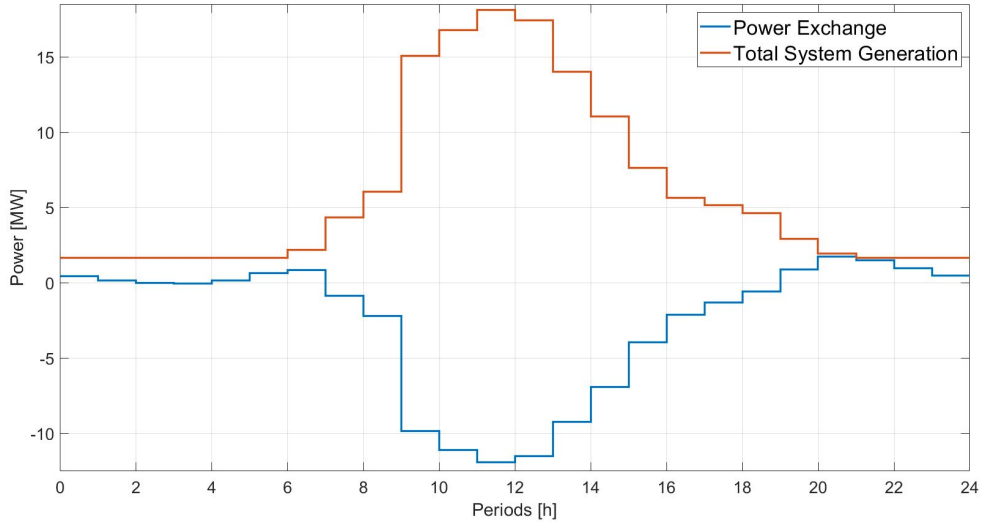

Figure 25: Total system's generation and power exchange in Case Study 2

The voltages present the same tendency as the generation data. During the night they have the same behaviour as explained in case study 1, but during the day they have to accommodate a much more considerable amount of power. Consequently in these hours, the network will have various buses reaching the voltage limit, and almost all of the network will have a higher voltage than the slack one, as reflected in Figure 26.

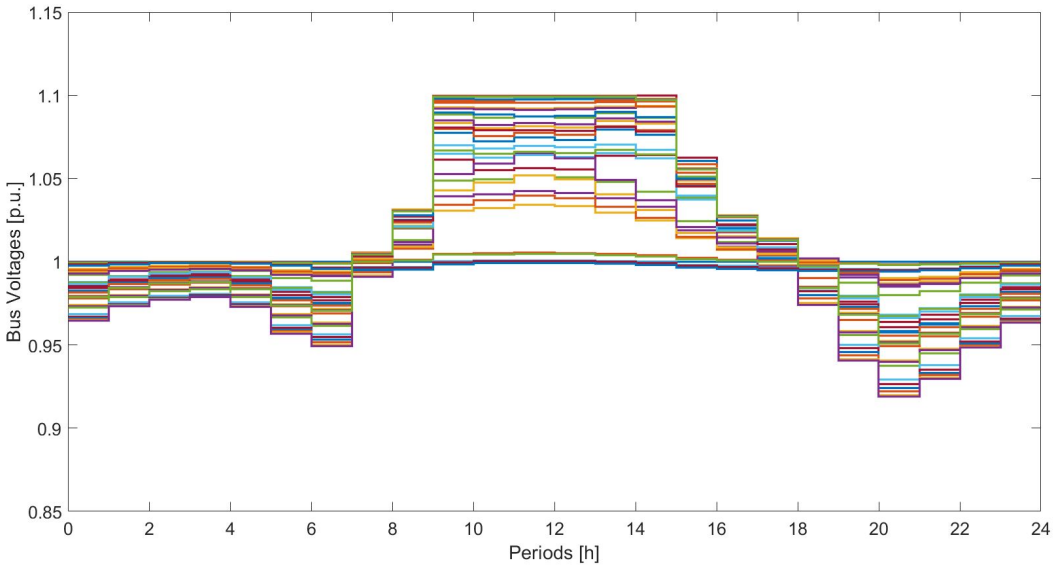

Figure 26: Buses Voltages Profiles throughout the day in p.u.

The following heat-map plot helps to understand the voltage behaviour better. It represents all the voltages in p.u. of all the buses in every period. During the night hours, all the nodes are below one p.u. (blue) and during the sunny hours, the colour green appears to represent higher voltages.

The main point of the Figure 27 is to highlight the behaviour of a specific branch of the feeder. As it can be seen, there is a blue stripe in the graph that breaks the global tendency of the system. In these buses 19 to 22, the voltages remain almost constant during the whole operation. These nodes present a different response because the generation available in this particular branch is not enough to fulfil the loads at any time and it has no solar panels. So they will import power no matter if it is day or night.

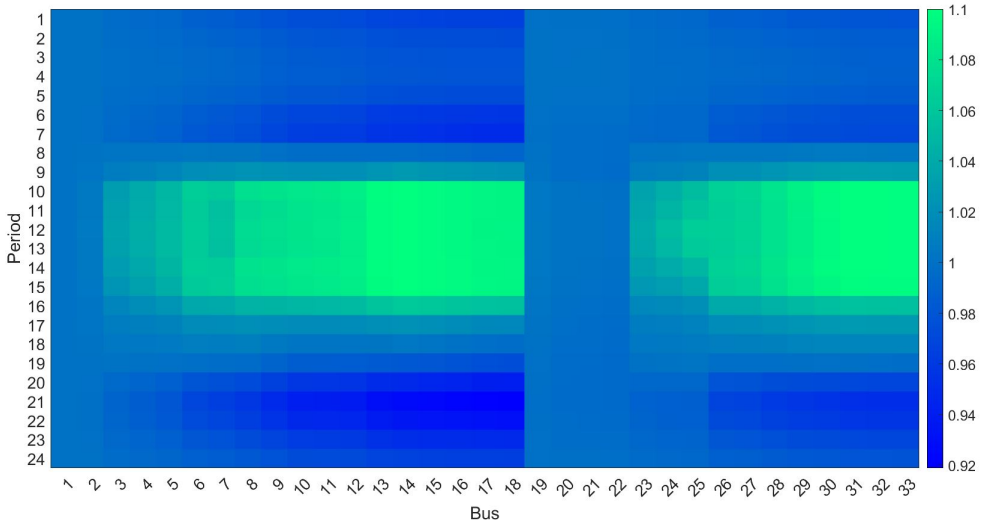

Figure 27: Buses Voltages Heat-map throughout the day in p.u.

The power losses are dramatically increased in this scenario. Because more than 60 MWh are transmitted through the slack node from all over the network, the electric currents are higher, and much power is dissipated in the lines during the day. The solver has considered this fact and decided that it was cheaper to lose power on the lines than to curtail electricity production. Therefore, the network approves having almost 10 MWh of energy losses. Nevertheless, from an operator point of view, this is not good. The network is not efficient, and it is harder for the installation to work so saturated. With this result, it is easily understood the need for an energy storage system able to give more liberty to the energy management to reduce these power losses. The profile is shown in figure 28.

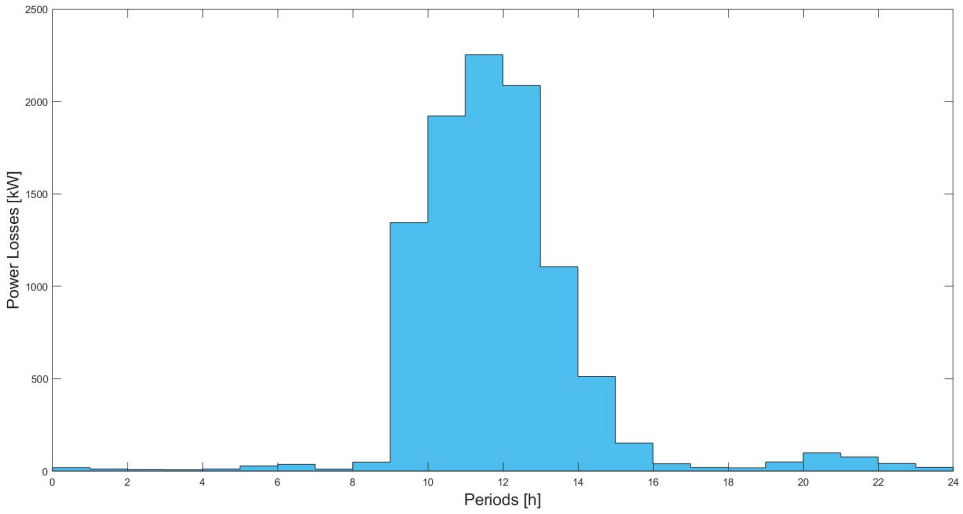

Figure 28: Total Power Losses throughout the day in p.u.

To conclude this case study, Table 17 contains a summary of the network results.

Op. Cost[€]	I max [p.u.]	V max [p.u.]	V min [p.u.]
-4,55674e+3	13,029	1,1	0,9189
	(From 2 to 1)	(Bus 14 and 31)	(Bus 18)
	(T = 12)	(T = 10 to 15)	(T = 21)
$PGdiesel$ [MWh]	$PGpv$ [MWh]	$PGslack$ [MWh]	PL [MWh]
33,88	113,965	-63,722	9,927

Table 17: Study Case Results

5.2.3 Case Study 3

With the previous two cases, it became evident the need for an energy storage system to improve a MVDN operation. The solar power swamps the network during the peak hours with an excess of energy that conditions all the system's operation. It increases all the systems' tensions and electric currents, pushing the installations to their limits and increasing the power losses. Furthermore, this thesis considered the possibility of exchanging power with the external grid, but if for any reason one day the trade is not available, the network would have to curtail much power.

So energy storage systems may have a very positive effect on the distribution network by reducing power losses, obtaining independence from the external grid, reducing the fuel generation, and smoothing the daily operation. All of this can be accomplished with the idea to store energy from the peak time to discharge it again in the off-peak time. This concept is mainly made possible by the use of photovoltaic generation.

There are many possibilities when it comes to storing energy. Technologies such as pumped hydro storage, CAES (Compressed Air Energy Storage), batteries, SMES (superconducting magnetic energy storage), Hydrogen storage with fuel cells, et cetera. [SA20] Nevertheless, this thesis will only consider the battery technology.

Six batteries will be distributed along the network on buses 8, 14, 24, 25, 30, and 31. As previously stated in section 5.1.7, this is the optimal battery location suggested in [AAK20]. The rated power of these batteries will be 4.480 kWh, with a 90 % efficiency when charging and discharging. The system's BESS can store up to 73,82 % of the peak hour photovoltaic generation

and up to 23,34 % of the energy total solar production.

The rest of the parameters will remain equal to the ones considered in case study 2, summed up in Figure 24 and Table 16.

Again, the solver used for this study in GAMS is the SCIP. The model consists of 9.889 variables and 12.648 equations. The solution provided by GAMS is exact, so the optimal solution is feasible to the non-relaxed problem. Hence the application of the solution recovery algorithm is not necessary because all the lines satisfy the equation (5.9).

$$l_{ijt} = \frac{P_{ijt}^2 + Q_{ijt}^2}{u_{it}}, \qquad \forall (i,j) \in \Omega \quad \forall t \in T \tag{5.9}$$

The generation output in this scenario, illustrated in Figure 29, is almost equal to the maximum generations plot. The solar power production is a little bit bigger than before since now it is not curtailing any. The diesel generation profile is also similar, but the generation during the peak hours has slightly increased. This increment is due to the fact that in the present scenario, the system is not as saturated as before and has some room left to increase this type of generation aiming to sell it to the external grid.

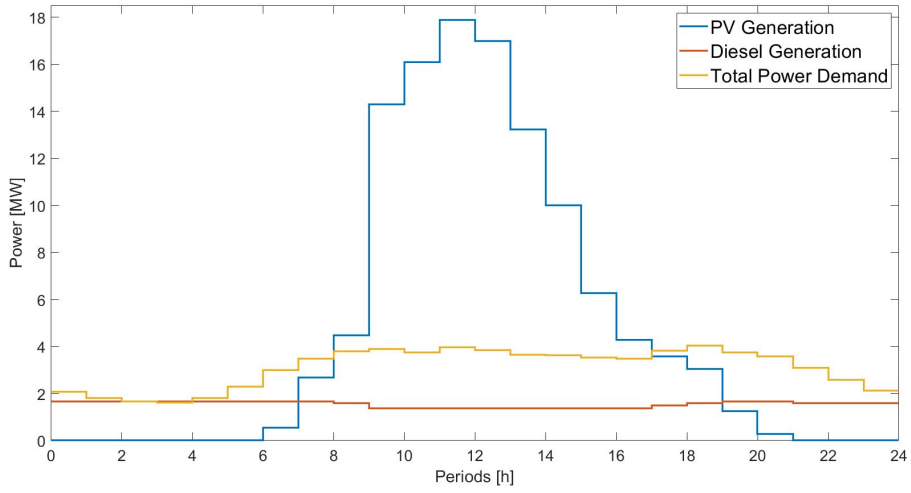

Figure 29: PV and Diesel Generation/Demand in Case Study 3

The following Figure 30 shows the evolution of the power exchange on the slack node. Adding batteries eliminates the purchase of electricity from the external grid, making the network completely independent. This is a very positive effect on the system. In this scenario, if the slack node connection failed, the network generation could still satisfy all the demand. Note that

there is a decrease in the peak energy sold but an overall increase in the power sold. Therefore, spacing the power sold reduces the peak electrical currents, which implies fewer power losses.

This plot also illustrates that it is cheaper to store solar energy for later than to sell it to buy more in the following hours. Hence, part of the generated power during solar hours now is stored for coming hours, so the power sold from 8 a.m to 6 p.m is reduced from 70,91 MWh to 60,3 MWh.

The batteries effect on the network makes the energy sold during peak hours more constant, thus it is more distributed during the hours. As a result, even the peak power generation does not coincide with the peak of the power exchanged. This more spread trade profile reduces the peak transmission of electricity, reducing power losses while storing energy for later.

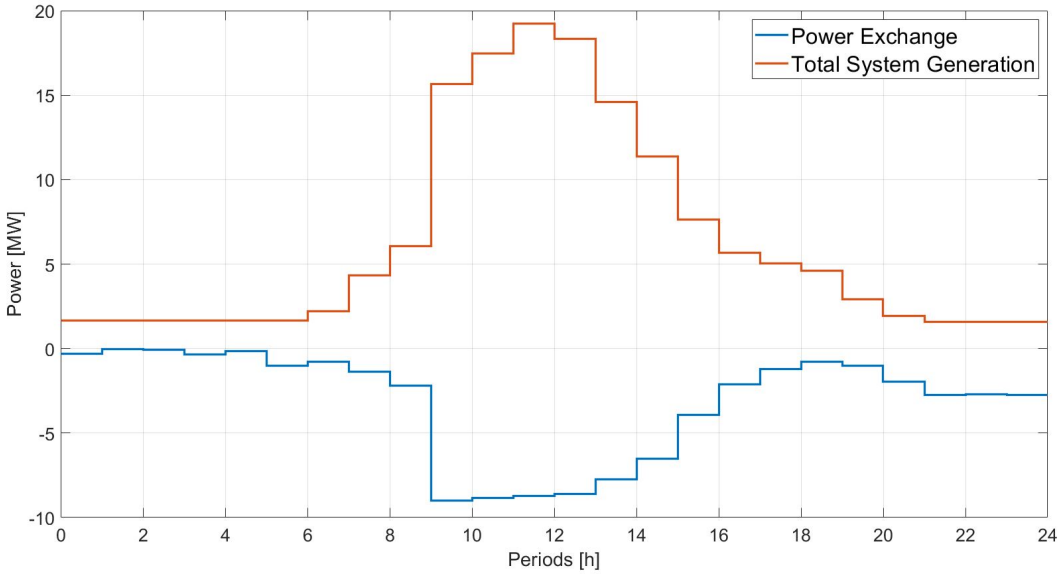

Figure 30: Total system's generation and power exchange in Case Study 3

The following Figure 31 representing the buses voltages is instrumental in explaining two factors. Firstly, what happens in the first eight periods where the network is selling power, but almost all the voltages are below the reference. And secondly, why the system's voltages decrease so much when the sun is fading away.

Although some power is leaving the network in the first eight hours, the voltages are lower than the reference. After analyzing the system's behaviour, what happens is that the only power leaving is produced from the diesel generator on bus 2. From node two downstream, all the directions are arranged to fulfil all the buses demand from the diesel generators and the stored

energy on the batteries. Furthermore, because generators and batteries are distributed along the lines, the voltages are set depending on the distance to those. In this scenario, the current directions are more chaotic than in the previous two cases.

This is also the reason why the voltages drop so much when the sun starts disappearing. The diesel generators and the stored energy on the batteries cover the system's loads less abundantly, and the voltages will adapt to the power coming from nodes distributed along the whole network while still selling some power.

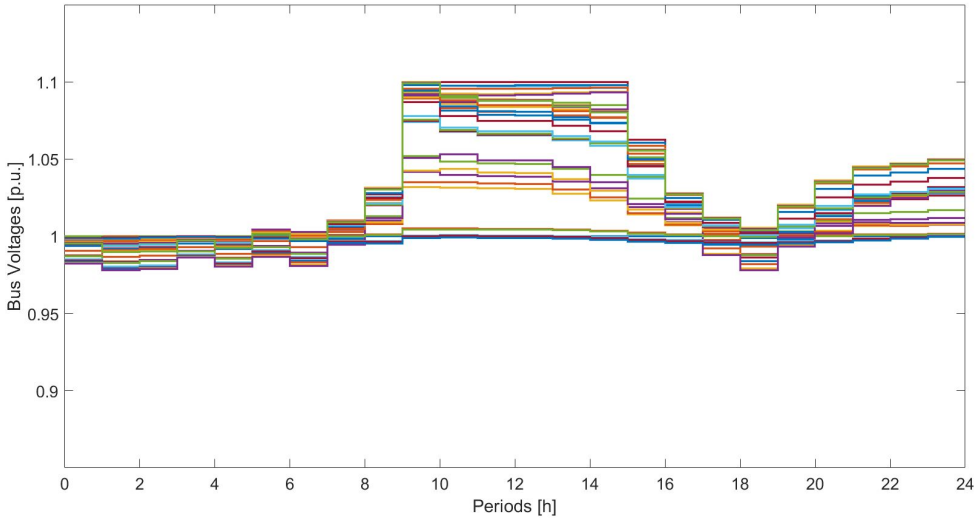

Figure 31: Buses Voltages Profiles throughout the day in p.u.

The next Figure 32 graphs how the global power losses of the network evolve. The reduction of the dissipated energy is one of the primary purposes of adding BESS, and it can be seen on this profile. The power losses with these six batteries have been reduced to 46,79 % of the previous scenario. This significant decrease is promoted by spreading out power sold to the grid.

It is also interesting to see how the batteries state of charge varies throughout the day. As can be seen in Figure 33, except for the battery on nodes 24 and 25, the batteries release their energy gradually during the first hours of the day at the pace marked by the system's demand until they are fully discharged. Then they recharge until full capacity to discharge all the stored energy gradually through the last hours of the day. As previously stated, the optimization will consider a one-day operation, ergo the batteries will not have any incentive to save power for the next day.

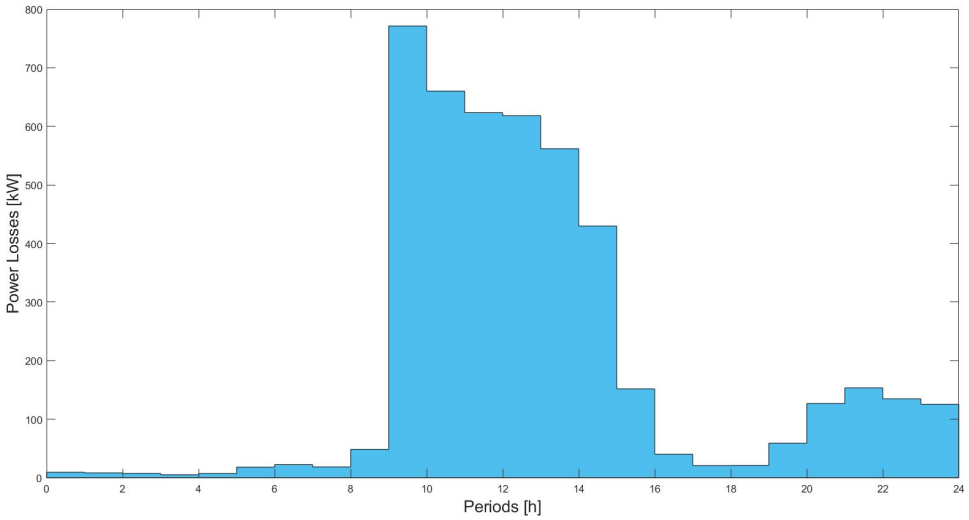

Figure 32: Total Power Losses throughout the day in p.u.

Batteries of nodes 24 and 25 are situated at the downstream nodes of a 4-bus branch. The only generator on those lines is on node 25, and its production is not enough to satisfy the four loads' demand and charge the batteries. This is the reason why those two devices present a different behaviour than the others. Concluding that the battery of node 24 or 25 should be relocated if it was to be useful to the network. Otherwise, it should not be installed.

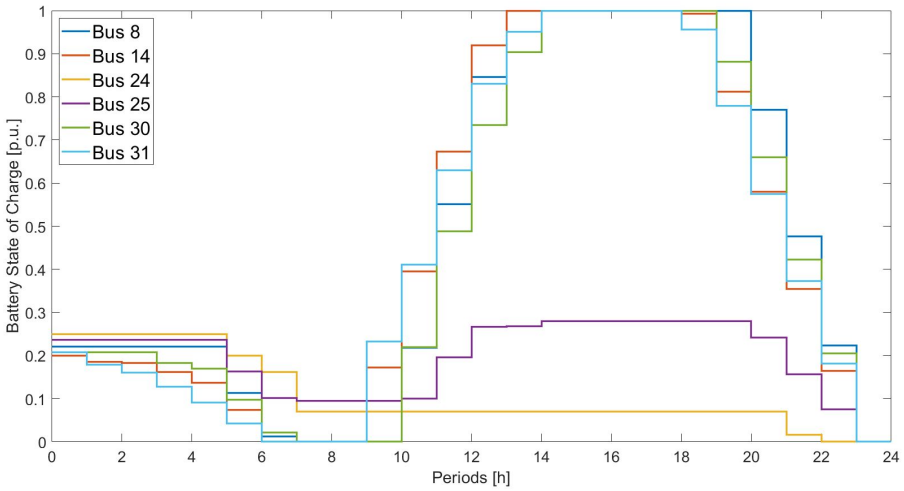

Figure 33: Batteries State of Charge throughout the day in p.u.

Another thing that must not be forgotten is that the batteries do not work with perfect efficiency. As defined in the specification of the parameters, these have a 90 % efficiency when charging and when discharging. So the reduction of power losses should not be lower than the energy dissipated on the electrochemical conversion.

In this case, the energy dissipated on the batteries is 4,88 MWh. Adding this value to the power losses gets 9,53 MWh of energy dissipated. It is a little bit lower than in the scenario with no batteries but still not enough to justify the implementation of this energy storage system.

Although energy dissipation is really important in this problem, the objective function is trying to minimize other variables. Thereby other solutions with fewer power losses may be feasible but are not the objective of the problem.

Therefore, the justification of these devices comes from two main factors. The first one being that the batteries convert the system into an auto-sufficient network. The second one from an objective value standpoint explained in the following paragraphs.

With the implementation of these devices, the objective function is reduced a 41,9 % compared to the scenario with no batteries. This is a very significant improvement on the daily operation of the distribution network that justifies the use of these systems.

The following Figure 34 sheds light on why the batteries charge and store energy during peak hours and discharge it later. This representation shows the total energy stored in the network in MWh with the electricity rates profile normalized and displaced to fit in the plot. As can be seen, when the electricity rates are the lowest, the energy storage system charges its devices, anticipating that the electricity is more expensive later. Saving this energy for succeeding hours allows it to make a more significant profit from renewable generation. This strategy is one of the main reasons why the operating costs in this scenario are so much lower than before.

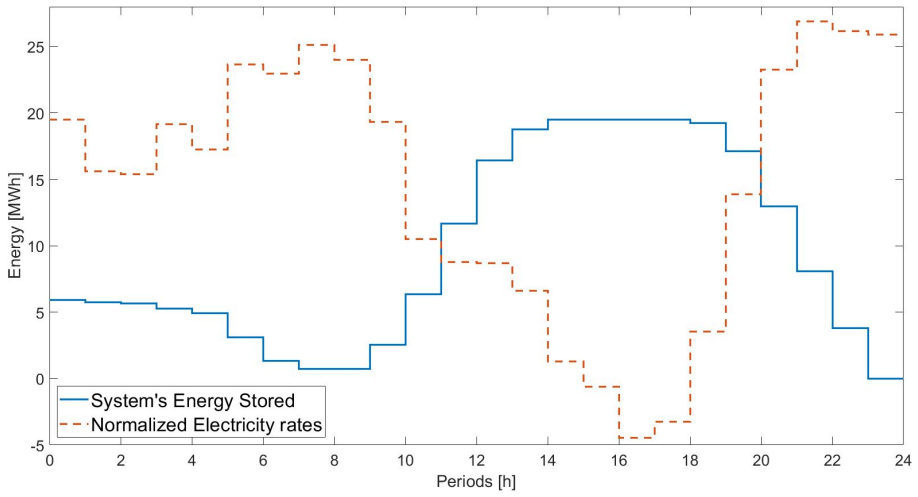

Figure 34: Total Energy Stored in the BESS throughout the day

To conclude this case study, Table 18 contains a summary of the network results.

Op. Cost[€]	I max [p.u.]	V max [p.u.]	V min [p.u.]
-6,4662e+3	9,004	1,1	0,9778
	(From 2 to 1)	(Bus 14 and 31)	(Bus 18)
	(T = 10)	(T = 10 to 15)	(T = 2)

$PGdiesel$ [MWh]	$PGpv$ [MWh]	$PGslack$ [MWh]	PL [MWh]
36,86	114,879	-74,98	4,66

Table 18: Study Case Results

6 Conclusions and Future Work

6.1 Conclusions

This thesis presents an optimization model that determines the operating states of an electrical power system for a daily demand forecast at hourly time fidelity. This formulation includes the technical and economic models of diesel generation, photovoltaic power production, and battery energy storage systems, as well as the grid behaviour.

The implementation requires three software: MATLAB, GAMS, and EXCEL. The use of these programs allows creating a highly adaptable model to different configurations, which can be used for almost any radial network of any size. With these environments, the optimal power flow problem is solved using the second-order cone relaxation.

A critical aspect that has been successfully addressed in this thesis is the fact that the model does not guarantee an exact solution. It happened in one case study, where the solution is not feasible to the non-relaxed problem. When this occurs, the operator must develop a strategy to find the non-relaxed optimal solution because the one given by the optimization does not satisfy the physical constraints. This is tackled with an algorithm based on a series of conditions demonstrated in the literature that, if fulfilled, guarantees an exact result. Because the operating costs function does not follow these conditions, an auxiliary objective function is developed that narrows down to the optimal solution through an iterative process.

This optimization problem is tested with the IEEE 33-Bus network on three different scenarios, each one as a continuation of the previous one. The batteries model is only simulated in the third case as an improvement of the second one.

The first one is a regular case where the diesel generation and the photovoltaic total generation capability barely cover the network's demand. However, because the solar power is concentrated in a few hours, the network is obligated to sell all the excess power in the peak hours to repurchase it later.

The second one poses the simulation of what would happen if the maximum solar generation increased. Because, contrary to the fuel production, increasing the solar electricity production does not have any direct cost to the network operation, the same case as before is simulated but

heavily increasing the rated power of the solar panels.

In this scenario, the network during the peak hours gets saturated with power, but instead of curtailing generation, it keeps increasing production by virtually increasing the current. It finds cheaper the cost of dissipating the power through the lines than to curtail power. Obviously, this solution is not physically possible and does not fulfil the apparent power equation of the lines. This is when the solution recovery algorithm kicks in, using the power losses as the auxiliary objective function and the operating cost as a restriction. After eleven iterations, finds the optimal feasible result to the non-relaxed problem.

Finally, in the third scenario, the model considers the same network data as before but adding six batteries spread out along the network. Theoretically, the energy storage systems add various advantages to the operation of a system with solar electricity production, which is corroborated in this study. The network becomes auto-sufficient and completely independent from the external grid and reduces almost by half the cost of the operation.

Where there is a fewer improvement than expected is in the systems' power losses. One of the main reasons for implementing the batteries was to reduce the power dissipated in the lines during peak hours. However, although these losses are reduced by half, if the problem takes into account the losses in the electrochemical conversion, the system losses do not decrease significantly. Nevertheless, the advantages that provide to the system's justify the implementation of this technology even though it does not solve the problem of power dissipation.

From the three scenarios can be seen that increasing the photovoltaic rated power reduces the operational cost of the network. This decrease in the objective function can justify the cost of purchasing, installing and maintaining this generation technology. If the sizing and sitting of the panels are done correctly, the installation presents an excellent opportunity to make a profit. This planning task requires a deep study since too many panels can saturate the network and rapidly decrease the network efficiency.

Another significant improvement in the system is the installation of batteries. They reduced almost by half the objective variable, storing energy from the peak hours to discharge it in less productive hours. This considerable reduction is made with the capacity of only storing a quarter of the solar production. Ergo these devices presented much potential in the network's operation. Moreover, they converted the network into an auto-sufficient system, not only from the

external grid but also between branches. This is a very positive improvement since, in radial networks, a disconnection in one node could imply the disconnection of all the downstream nodes.

The solution recovery algorithm presents a very practical tool for optimal power flows problems based on the Branch Flow Model that incorporates the second-order cone relaxation. In most cases, these optimizations do not present a model that guarantees the feasibility of the solution to the non-relaxed problem. The algorithm developed in this thesis provides the tool to find the optimal solution that makes physical sense for all kinds of different objective functions.

6.2 Future Work

There are several ideas to increase the accuracy of the model. In future work, using a better solver such as CPLEX enables more non-linear equations with less computing time. In this thesis, the diesel generator economic model had to be linearized to decrease the computing time. Although the approximation is assumable in the problem, using quadratic functions would slightly increase the accuracy.

Another interesting and complex idea for future work is determining the optimal sitting and sizing of the different technologies applied. In this project, the sitting and sizing of the diesel and photovoltaic generators, along with the batteries, was based on articles from the literature. However, developing an algorithm to determine those parameters could significantly increase the network efficiency.

The last two proposals to continue the research of this thesis are to extend the time set so that the batteries may consider storing energy for the next day, and operating some parameters under uncertainty. The scenarios assumed that all the data inputs were deterministic, but in reality some parameters do not always follow the previsions.

7 Economic Analysis

7.1 Introduction

This section presents the costs associated with the realization of this project. This is a simulation and programming project, so the budget elements are limited to the developer's work and the resources used.

7.2 Project Budget

The economic analysis will be divided into two parts. The first will consider the project's development time and the second will examine the material and software needed.

The working time invested in this project adds up to 450 hours, distributed in the following tasks: conceptual development and investigation, programming and simulations, and redaction. Table 19 illustrates the workload distribution.

Description	Hours	Price/hour	Total
Conceptual development and investigation	130	45 [€/h]	5.850 [€]
Programming and simulations	200	45 [€/h]	9.000 [€]
Redaction	120	45 [€/h]	5.400 [€]
Subtotal			20.250 [€]

Table 19: Development time budget

The software and hardware needed are listed in table 20.

Description	Unit/price	Units	Total
Asus Rog Strix G15	1.250 [€]	0,25	312,5 [€]
GAMS ®	640 [€]	1	640 [€]
MATLAB ®	250 [€]	1	250 [€]
Microsoft Office ®	70 [€]	0,5	35 [€]
Subtotal			1.237,5 [€]

Table 20: Hardware and Software budget

So table 21 shows the total budget.

Description	Price
Workload	20.250 [€]
Hardware and Software	1.237,5 [€]
Operating costs (8 %)	1.719 [€]
Subtotal	23.206,5 [€]
I.V.A. (21 %)	4.873,4 [€]
Total	28.080 [€]

Table 21: Total Project budget

This budget has a validity of 4 months from the signing.

Ignasi Ventura Nadal, 17/06/2021

8 Environmental Impact

All the studies of this project have been done from simulations, and no equipment, except for the typical office material, was used for its realization. Hence the impact of this project is meagre and it is limited to the use of electric devices and air conditioning. This assessment can only take into account the power consumption of a computer, a computer mouse, and an internet connection, along with lighting and heating of the working space.

The environmental impact of implementing some of the technologies modelled in the distribution networks is a pervasive and complex subject and does not apply to this thesis.

Bibliography

[Ach+04] Enrique Acha et al. *FACTS: Modelling and Simulation in Power Networks*. Wiley, 2004. ISBN: 0470852712.

[Age20] U.S. Energy Information Agency. *Electricity Explained*. Last accessed 22 March 2021. 2020. URL: https://www.eia.gov/energyexplained/electricity/use-of-electricity.php/.

[Ahn+13] Seon-Ju Ahn et al. "Power Scheduling of Distributed Generators for Economic and Stable Operation of a Microgrid". In: (Mar. 2013). DOI: 10.1109/TSG.2012.2233773.

[Alb19] Mohammed Albadi. "Power Flow Analysis". In: Mar. 2019. ISBN: 978-1-78923-869-3. DOI: 10.5772/intechopen.83374.

[AAK20] Ahmed Alzahrani, Hussain Alharthi, and Muhammad Khalid. "Minimization of Power Losses through Optimal Battery Placement in a Distributed Network with High Penetration of Photovoltaics". In: *Energies* 13.1 (2020). ISSN: 1996-1073. DOI: 10.3390/en13010140. URL: https://www.mdpi.com/1996-1073/13/1/140.

[Ass20] World Nuclear Association. *Renewable Energy and Electricity*. Last accessed 21 March 2021. 2020. URL: https://www.world-nuclear.org/information-library/energy-and-the-environment/renewable-energy-and-electricity.aspx/.

[AES15] Ahmed Awad, Tarek EL-Fouly, and M.M.A. Salama. "Optimal ESS Allocation for Load Management Application". In: *IEEE Transactions on Power Systems* 30 (Jan. 2015), pp. 327–336. DOI: 10.1109/TPWRS.2014.2326044.

[BW89] M E Baran and F F Wu. "Optimal sizing of capacitors placed on a radial distribution system". In: *IEEE Trans. Power Del.; (United States)* (Jan. 1989). DOI: 10.1109/61.19266. URL: https://www.osti.gov/biblio/6373292.

[Ber14] J.R. Berendero. "Funciones convexas y optimización convexa". In: (2014).

[Bha16] Mihir Bhagat. "Convex Guidance for Envisat Rendezvous". PhD thesis. Feb. 2016.

[Boo+20] Panyawoot Boonluk et al. "Optimal Siting and Sizing of Battery Energy Storage Systems for Distribution Network of Distribution System Operators". In: *Batteries* 6 (Nov. 2020), p. 56. DOI: 10.3390/batteries6040056.

[BV04] Stephen Boyd and Lieven Vandenberghe. *Convex Optimization*. Cambridge University Press, 2004. ISBN: 9780511804441.

[CZ17] Yu Cheng and Chengwei Zhang. "Configuration and operation combined optimization for EV battery swapping station considering PV consumption bundling".

In: *Protection and Control of Modern Power Systems* 2 (Dec. 2017). DOI: 10.1186/s41601-017-0056-y.

[Cig14] Cigré. "Benchmark Systems for Network Integration of Renewable and Distributed Energy Resources". In: (Apr. 2014). DOI: 10.1016/S0142-0615(03)00046-2.

[Clo+19] Josep Andreu Clos et al. "Optimal Operation of Isolated Microgrids Considering Frequency Constraints". In: *Applied Sciences* 9 (Jan. 2019), p. 223. DOI: 10.3390/app9020223.

[DC19] Indrajit Das and Claudio A. Cañizares. "Renewable Energy Integration in Diesel-Based Microgrids at the Canadian Arctic". In: (Sept. 2019). DOI: C18-SD-63-03.

[Ene] Institute of Energy Research. *History of Electricity*. Last accessed 16 March 2021. URL: https://www.instituteforenergyresearch.org/history-electricity/.

[Eur18] Council of European Energy Regulators. "Status Review of Renewable Support Schemes in Europe for 2016 and 2017". In: (Dec. 2018). DOI: C18-SD-63-03.

[FL12] Masoud Farivar and Steven H. Low. "Branch Flow Model: Relaxations and Convexification". In: *CoRR* abs/1204.4865 (2012). arXiv: 1204.4865. URL: http://arxiv.org/abs/1204.4865.

[fL12] Eduardo de francesco and Fabio Leccese. "Risks analysis for already existent electric lifelines in case of seismic disaster". In: (May 2012). DOI: 10.1109/EEEIC.2012.6221490.

[Gar04] Francisco F. Garcés. "Electric Power: Transmission and Generation Reliability and Adequacy". In: *Encyclopedia of Energy*. Ed. by Cutler J. Cleveland. New York: Elsevier, 2004, pp. 301–308. ISBN: 978-0-12-176480-7. DOI: https://doi.org/10.1016/B0-12-176480-X/00514-3. URL: https://www.sciencedirect.com/science/article/pii/B012176480X005143.

[GK17] Yogi Goswami and Frank Kreith. *Energy Conversion*. CRC Press, 2017. ISBN: 9 781 466584822.

[Işı15] Tunahan Işık. "Solar Cells review". PhD thesis. Jan. 2015. DOI: 10.13140/RG.2.1.4298.6404.

[JH08] Marijn Jongerden and B. Haverkort. "Battery Modeling". In: *CTIT Report* (Jan. 2008).

[LY08] David G. Luenberger and Yinyu Ye. *Linear and Nonlinear Programming*. Springer, 2008. ISBN: 978 0 387 74502 2.

[Mas18] Eduard Bullich Massagué. "Feeder flow control and operation in large scale photovoltaic power plants and microgrids". PhD thesis. U. Politècnica de Catalunya, 2018.

[Mom09] James A. Momoh. *Electric Power System Applications of Optimization*. CRC Press, 2009. ISBN: 9781420065862.

[RAW14] Pekka Ruuska, Antti Aikala, and Robert Weiss. "Modelling Of Photovoltaic Energy Generation Systems". In: May 2014, pp. 651–656. ISBN: 9780956494481. DOI: 10.7148/2014-0651.

[SG20] Pawan Saini and Lata Gidwani. "Optimal siting and sizing of battery in varying PV generation by utilizing genetic algorithm in distribution system". In: *2020 21st National Power Systems Conference (NPSC)*. 2020, pp. 1–6. DOI: 10.1109/NPSC49263.2020.9331765.

[SS04] M. Selvan and Shanti Swarup. "Object-oriented power system analysis". In: *Journal of the Indian Institute of Science* 84 (Sept. 2004), pp. 141–154.

[SA20] Kamaruzzama Sopian and Amr Al-Hinai. "Review of energy storage services, applications, limitations, and benefits". In: *Energy Reports* 6 (Aug. 2020). DOI: 10.1016/j.egyr.2020.07.028.

[Sor17] Alireza Soroudi. *Power System Optimization Modeling in GAMS*. Springer, 2017. ISBN: 9 783319872971.

[Swa17] Bhargav Prasanna Swaminathan. "Operational Planning of Active Distribution Networks – Convex Relaxation under Uncertainty". PhD thesis. Université Grenoble Alpes, 2017.

[Vic19] Marc Antoni Fiol Vich. "Optimització del flux de potència en xarxes de distribució intel·ligents". MA thesis. Universitat Politècnica de Catalunya, 2019.